BBA - Molecular and Cell Biology of Lipids

Exploring the endocannabinoidome in genetically obese (ob/ob) and diabetic (db/db) mice: links with inflammation and gut microbiota.

--Manuscript Draft--

Manuscript Number:	
Article Type:	Regular Paper
Keywords:	Endocannabinoids Liver Adipose tissue Obesity Diabetes Microbiome
Corresponding Author:	Vincenzo Di Marzo Centre de recherche de l'Institut universitaire de cardiologie et de pneumologie de Québec Quebec City, Quebec CANADA
First Author:	Francesco Suriano, Doctor
Order of Authors:	Francesco Suriano, Doctor
	Claudia Manca, Doctor
	Nicolas Flamand, Professor
	Clara Depommier, Doctor
	Matthias Van Hul, Doctor
	Nathalie M. Delzenne, Professor
	Cristoforo Silvestri, Professor
	Patrice D. Cani, Professor
	Vincenzo Di Marzo, Professor
Abstract:	Background: Obesity and type 2 diabetes are two interrelated metabolic disorders characterized by insulin resistance and a mild chronic inflammatory state. We previously observed that leptin (ob/ob) and leptin receptor (db/db) knockout mice display a distinct inflammatory tone in the liver and adipose tissue. The present study aimed at investigating whether alterations in these tissues of the molecules belonging to the endocannabinoidome (eCBome), an extension of the endocannabinoid (eCB) signaling system, whose functions are important in the context of metabolic disorders and inflammation, could reflect their different inflammatory phenotypes. Results: The basal eCBome lipid and gene expression profiles, measured by targeted lipidomics and qPCR transcriptomics, respectively, in the liver and subcutaneous or visceral adipose tissues, highlighted a differentially altered eCBome tone, which may explain the impaired hepatic function and more pronounced liver inflammation remarked in the ob/ob mice, as well as the more pronounced inflammatory state observed in the subcutaneous adipose tissue of db/db mice. In particular, the levels of linoleic acid-derived endocannabinoid-like molecules, of one of their 12-lipoxygenase metabolites and of Trpv2 expression, were always altered in tissues exhibiting the highest inflammation. Correlation studies suggested the possible involvement of some gut microbiota bacterial taxa, whose respective absolute abundances were significantly different between ob/ob and the db/db mice. Conclusions: The present findings emphasize the possibility that bioactive lipids and the respective receptors and enzymes belonging to the eCBome may sustain the tissue-dependent inflammatory state that characterize obesity and diabetes, possibly in relation with gut microbiome alterations.
Suggested Reviewers:	Pal Pacher NIH: National Institutes of Health pacher@mail.nih.gov

	Expertise in understanding the role of endocannabinoids and related mediators, and their metabolic pathways during tissue injury
	Mireille Alhouayek Université catholique de Louvain: Universite Catholique de Louvain mireille.alhouayek@uclouvain.be Expertise in the link between endocannabinoids and inflammation
	Renger Witkamp Wageningen UR: Wageningen University & Research renger.witkamp@wur.nl His research focuses on bioactive lipids and their role in obesity and inflammation
	PierLuigi Plastina Università della Calabria: Universita della Calabria p.plastina@unical.it His research focuses in the study of bioactive lipids and their role in inflammation and immunomodulatory activity.

Exploring the endocannabinoidome in genetically obese (*ob/ob*) and diabetic (*db/db*) mice: links with inflammation and gut microbiota.

Francesco Suriano[1, #], Claudia Manca[2,3, #, $], Nicolas Flamand[2], Clara Depommier[1], Matthias Van Hul[1], Nathalie M. Delzenne[1], Cristoforo Silvestri[2,3], Patrice D. Cani[1, *], Vincenzo Di Marzo[2,3,4, *].

[1]Metabolism and Nutrition Research group, Louvain Drug Research Institute (LDRI), Walloon Excellence in Life Sciences and BIOtechnology (WELBIO), UCLouvain, Université catholique de Louvain, Av. E. Mounier, 73 B1.73.11, 1200 Brussels, Belgium.

[2]Quebec Heart and Lung Institute Research Centre, Université Laval, Quebec City, QC G1V 0A6, Canada.

[3]Centre NUTRISS, Institute of Nutrition and Functional Foods, Université Laval, Quebec City, QC G1V 0A6, Canada.

[4]Endocannabinoid Research Group, Institute of Biomolecular Chemistry, Consiglio Nazionale delle Ricerche, 80078 Pozzuoli, Italy.

[#] These authors equally contributed to this work

[*] To whom correspondence should be addressed:

Professor Patrice D. Cani, patrice.cani@uclouvain.be (phone number: +32 27647397); Professor Vincenzo Di Marzo, vincenzo.dimarzo@criucpq.ulaval.ca (phone number: 418 656-8711 ext. 7263)

$ current address: Department of Biomedical Science, University of Cagliari, 09042 Monserrato, Italy

Short title: eCBome and inflammation: learning from *ob/ob* and *db/db* mice

Funding sources: This work was supported by the Fonds de la Recherche Scientifique (FNRS FRFS-WELBIO) under the grants WELBIO-CR-2017C-02 and WELBIO-CR-2019C-02R, the Funds Baillet-Latour under the grant “Grant For Medical Research 2015”. C.S. and N.F. are associated to the Canada Excellence Research Chair on the microbiome-endocannabinoidome axis in metabolic health, held by V.D. and funded by the Canadian Federal Tri-Agency.

Abbreviations

The abbreviations for endocannabinoid and related lipid mediator, receptors and enzymes are listed in Supplemental Table S1 and S2.

2-MAGs, 2-acylglycerols; AA, arachidonic acid; Acaca, acetyl-Coenzyme A carboxylase alpha; Adgre1, adhesion G Protein-Coupled Receptor E1; Baat, bile acid-Coenzyme A: amino acid N-acyltransferase; CAconc, cholic acid concentration; CB1, cannabinoid receptor type 1; CB2, cannabinoid receptor type 2; Ccl2, chemokine (C-C motif) ligand 2; Cd14, CD14 antigen; Cd163, CD163 antigen; Cd68, CD68 antigen; Cebpa, CCAAT/enhancer binding protein (C/EBP) alpha; CHOLcont, cholesterol content; CLSn, crown-like structures number; Col1a1, collagen type I alpha 1; Cpt1a, carnitine palmitoyltransferase 1a liver; Cyp27a1, cytochrome P450 family 27 subfamily a polypeptide 1; Cyp7a1, cytochrome P450 family 7 subfamily a polypeptide 1; Cyp8b1, cytochrome P450 family 8 subfamily b polypeptide 1; eCB, endocannabinoid; eCBome, endocannabinoidome; FM, fat mass; GM, gut microbiota; GPR, G-protein-coupled receptor; Hnf4a, hepatic nuclear factor 4 alpha; Il1b, interleukin 1 beta; Itgax, integrin alpha X; LPS, lipopolysaccharide; LPSconc, lipopolysaccharide concentration; NAEs, N-acylethanolamines; Nlrp3, NLR family pyrin domain containing 3; Oatp1b2, solute carrier organic anion transporter family member 1b2; Ptgs2, prostaglandin-endoperoxide synthase 2; Slc10a1, solute carrier family 10 (sodium/bile acid cotransporter family) member 1; Slc27a5, solute carrier family 27 (fatty acid transporter) member 5; Slc51b, solute carrier family 51 beta subunit; TGcont, triglycerides content; Tgfb1, transforming growth factor beta 1; TLcont, total lipids content; Trl2, toll-like receptor 2; Trl4, toll-like receptor 4; Trl5, toll-like receptor 5; TRPV1, transient receptor potential cation channel subfamily V member 1.

Abstract

Background: Obesity and type 2 diabetes are two interrelated metabolic disorders characterized by insulin resistance and a mild chronic inflammatory state. We previously observed that leptin (*ob/ob*) and leptin receptor (*db/db*) knockout mice display a distinct inflammatory tone in the liver and adipose tissue. The present study aimed at investigating whether alterations in these tissues of the molecules belonging to the endocannabinoidome (eCBome), an extension of the endocannabinoid (eCB) signaling system, whose functions are important in the context of metabolic disorders and inflammation, could reflect their different inflammatory phenotypes.

Results: The basal eCBome lipid and gene expression profiles, measured by targeted lipidomics and qPCR transcriptomics, respectively, in the liver and subcutaneous or visceral adipose tissues, highlighted a differentially altered eCBome tone, which may explain the impaired hepatic function and more pronounced liver inflammation remarked in the *ob/ob* mice, as well as the more pronounced inflammatory state observed in the subcutaneous adipose tissue of *db/db* mice. In particular, the levels of linoleic acid-derived endocannabinoid-like molecules, of one of their 12-lipoxygenase metabolites and of *Trpv2* expression, were always altered in tissues exhibiting the highest inflammation. Correlation studies suggested the possible involvement of some gut microbiota bacterial taxa, whose respective absolute abundances were significantly different between *ob/ob* and the *db/db* mice.

Conclusions: The present findings emphasize the possibility that bioactive lipids and the respective receptors and enzymes belonging to the eCBome may sustain the tissue-dependent inflammatory state that characterize obesity and diabetes, possibly in relation with gut microbiome alterations.

Keywords: Endocannabinoids, Liver, Adipose tissue, Lipid signaling, Obesity, Diabetes, Microbiome

1. Introduction

During the last years, there has been an upsurge of interest in the expanded endocannabinoid (eCB) system - known as the endocannabinoidome (eCBome) - which comprises several bioactive lipid families biochemically related to the endocannabinoids, their receptors, and metabolic enzymes [1, 2]. The eCBome is widely distributed in various tissues and organs (e.g., brain, liver, intestine, and adipose tissues), and owes its importance to its ability to modulate different physiological functions such as the regulation of glucose and lipid metabolism, food intake, neuroprotection, and inflammation, among others [3-5].

The two best characterized endocannabinoids are the arachidonic acid (AA) derivatives, *N*-arachidonoylethanolamine, also known as anandamide (AEA), and 2-arachidonoylglycerol (2-AG). They belong respectively to two large distinct families of lipids, the *N*-acylethanolamines (NAEs), and the 2-acylglycerols (2-MAGs). Besides AEA, the NAE family also includes *N*-palmitoylethanolamine (PEA), *N*-stearoylethanolamine (SEA), *N*-oleoylethanolamine (OEA), *N*-linoleylethanolamine (LEA), *N*-eicosapentanoylethanolamine (EPEA), and *N*-docosahexanoylethanolamine (DHEA), while the 2-MAG family encompasses 2-oleoylglycerol (2-OG), and 2-linoleoylglycerol (2-LG), among others. Within their respective families, AEA and 2-AG are the only truly potent and efficacious endogenous agonists of the cannabinoid (CB) receptor type 1 (CB_1) and 2 (CB_2). In addition to the CB receptors, both endocannabinoids can bind and activate the transient receptor potential cation channel subfamily V member 1 (TRPV1). Of note, AEA is a weak agonist of the peroxisome proliferator-activated receptor (PPAR) γ [6, 7]. On the other hand, the other NAEs and 2-MAGs act with varying efficacies at other receptors such as PPARα or G-protein-coupled receptors 55 (GPR55), 119 (GPR119) and 110 (GPR110) [6]. The levels of endocannabinoids and related mediators are fine-tune regulated by the activity of their synthesizing and degrading enzymes [8]. However, studies carried out over the last years have revealed a high degree of redundancy of the metabolic pathways and the corresponding enzymes of these lipids, further highlighting the complexity of the eCBome. Thus, attempting to predict changes in eCBome mediator tissue concentrations based on the observed alterations in the expression of corresponding anabolic and catabolic enzymes is often challenging [9]. Furthermore, it is known that the concentrations of the endocannabinoids-like molecules are also regulated by

the availability of their ultimate phospholipid precursors and, hence, by the dietary intake of the corresponding fatty acids [10, 11].

In the context of metabolic disorders, several studies demonstrated the existence of an association between altered levels or activation of eCB signaling at CB1 receptors and the development of different pathological conditions such as obesity and type 2 diabetes [11-16], hepatic disorders (i.e., steatosis) [17, 18], and intestinal/adipose tissue inflammation [19, 20]. Conversely, several pieces of evidence suggest that activation of other eCBome receptors, such as CB_2, PPARα and γ, GPR110, and GPR119 promote important anti-inflammatory and/or incretin-like effects [21, 22], which can be exploited to improve insulin sensitivity [23]. Other eCBome targets such as TRPV1 and GPR55 instead play both pro-inflammatory and insulin-sensitizing actions [22, 24]. Thus, the functional complexity of the eCBome, and its capacity to differently orchestrate metabolic pathways in different organs and tissues depending on the interplay between ligands and receptors, need further clarification.

We have previously shown that genetically obese (*ob/ob*) and diabetic (*db/db*) mice exhibit a distinct gut microbiota (GM) compositions and different Gram-negative bacteria-derived lipopolysaccharide (LPS) levels [25]. We also described that the inflammatory tone of these mice depends on the organ under investigation, with the *ob/ob* model having a more altered hepatic inflammation, while the *db/db* model was characterized by a more inflamed adipose tissue [25]. Our data thus emphasized that the development of obesity and diabetes is specifically organ-dysfunction related. In the present work, we aimed at investigating whether tissue-specific eCBome signaling is associated with the distinct inflammatory phenotypes characterizing *ob/ob* and *db/db* mice. Furthermore, given the existence of a bi-directional relationship between the GM and the eCBome [5, 6], we investigated whether the observed differential alterations in the eCBome tone correlate with changes in the composition/function of the GM.

2. Materials and Methods

2.1 Tissues

The liver and the two adipose tissue depots, i.e., subcutaneous adipose tissue (SAT), and visceral adipose tissue (VAT) used in this study to explore the eCBome tone originated from the same mice used in a previous study and extensively phenotyped in Suriano et al., [25]. All mouse experiments were approved by and performed in accordance with the guideline of the local ethics committee (Ethics committee of the Université catholique de Louvain for Animal Experiments specifically approved this study that received the agreement number 2017/UCL/MD/005). Housing conditions were specified by the Belgian Law of 29 May 2013, regarding the protection of laboratory animals (agreement number LA1230314).

2.2 Lipid extraction and HPLC-MS/MS for the analysis of eCBome mediators

Lipids were extracted from tissue samples according to the Bligh and Dyer method [26]. Briefly, about 10mg of liver and adipose tissues were sampled and homogenized in 1ml of a 1:1 Tris-HCl 50mM pH 7: methanol solution containing 0.1M acetic acid and 5ng of deuterated standards. 1ml of chloroform was then added to each sample, which were then vortexed for 30 seconds and centrifuged at 3000×g for 5 minutes. The organic phase was collected and another 1 ml of chloroform was added to the inorganic one. This was repeated twice to ensure the maximum collection of the organic phase. The organic phases were pooled and evaporated under a stream of nitrogen and then suspended in 50µl of mobile phase containing 50% of solvent A (water + 1mM ammonium acetate + 0,05% acetic acid) and 50% of solvent B (acetonitrile/water 95/5 + 1mM ammonium acetate + 0.05% acetic acid). 40µl of each sample were finally injected onto an HPLC column (Kinetex C8, 150 × 2.1mm, 2.6µm, Phenomenex) and eluted at a flow rate of 400µl/min using a discontinuous gradient of solvent A and solvent B [27]. Quantification of eCBome-related mediators (supplemental Table S1), was carried out by HPLC system interfaced with the electrospray source of a Shimadzu 8050 triple quadrupole mass spectrometer and using multiple reaction monitoring in positive ion mode for the compounds and their deuterated homologs.

In the case of unsaturated monoacylglycerols, the data are presented as 2-monoacylglycerols (2-MAGs) but represent the combined signals from the 2- and 1(3)-isomers since the latter are most likely generated from the former via acyl migration from the *sn*-2 to the *sn*-1 or *sn*-3 position.

2.3 RNA isolation, Reverse Transcription and qPCR-based TaqMan Open Array

Total RNA was prepared from collected tissues using TriPure reagent (Roche). Quantification and integrity analysis of total RNA was performed by running 1µl of each sample on an Agilent 2100 Bioanalyzer (Agilent RNA 6000 Nano Kit, Agilent, Santa Clara, CA, USA). All samples had a RNA integrity number (RIN) above 6. cDNA was prepared by reverse transcription of 1µg total RNA using a Reverse Transcription System Kit (Promega, Madison, Wisconsin, USA).

Sixty-five nanograms of starting RNA were used to evaluate the expression of the 52 eCBome-related genes and 4 housekeeping genes (supplemental Table S2) using a custom-designed qPCR-based TaqMan Open Array on a QuantStudio 12K Flex Real-Time PCR System (Thermo Fisher Scientific, CA, USA) following the manufacturer's instructions. Samples were analyzed randomly. mRNA expression levels were calculated from duplicate reactions using the $2^{-\Delta\Delta Ct}$ method as calculated by CFX Maestro Software (Bio-Rad) and are represented as fold change with respect to baseline within each tissue. *Rps 13* was used as reference gene.

2.4 Correlation analysis

As previously described [28], correlation analysis between two data sets of variables were performed using the R package 'psych' (version 2.0.9). Based on the normality of the data distribution, a parametric test (i.e., Pearson) which assumes a normal distribution, or a non-parametric test (Spearman) which assumes a non-normal distribution of the data were used. In detail, Pearson's rank test and the Bonferroni's adjustment were used when correlating metabolic parameters with the eCBome, whereas Spearman's rank test and Holm's adjustment were used when correlating the bacterial taxa with the eCBome. All statistical analyses were performed on RStudio (version 3.6.3, Rstudio Team, Boston, MA, USA).

2.5 Statistical analysis

Data are presented as the mean±standard error of the mean (S.E.M), as specified in the individual tables and figures. The differences between the groups were determined using a One-Way ANOVA followed by Tukey's post hoc test on ΔΔdCt and on fmol/mg tissue for gene expression levels and mediator levels respectively. Only statistically significant differences between *ob/ob* and *db/db* mice were reported. The differences between experimental groups were considered statistically significant with $P \leq 0.05$ and represented as follows: * $P \leq 0.05$, ** $P \leq 0.01$, *** $P \leq 0.005$, **** $P \leq 0.001$. Data were analyzed using GraphPad Prism version 8.00 for Windows (GraphPad Software). The presence of outliers was assessed using the Grubbs test.

3. Results

3.1 Different eCBome profiles in the liver of ob/ob and db/db mice

We previously showed that *ob/ob* mice are characterized by a more pronounced inflammatory response in the liver as compared to *db/db* mice[25]. Looking for potential mechanisms and causal factors, we found that the two mutant models display distinct hepatic bile acids profiles and gut microbiota composition [25]. Since there is a cross-talk between the gut microbiota and bioactive lipids belonging to the eCBome, which have been implicated in several physiological and pathological conditions [5, 13, 29], we wondered whether the different inflammatory tones were also associated with differential eCBome profiles. Accordingly, we measured the concentration of a panel of eCBome-related mediators in tissues from the mice used in the previous study [25], and performed transcriptomic analysis looking at the gene expression of their corresponding anabolic and catabolic enzymes, as well as their receptors (Figure 1A, B and supplemental Table S3). Although several alterations in both genetic models were found, we discuss hereafter only those that were significantly different between *ob/ob* and *db/db* mice and hence might underlie the observed differences in inflammation-related indicators. Other alterations noted in the hepatic tissue are shown in supplemental Table S3. Concerning the eCBs and related molecules (Figure 1A), we did not find any significant change in the hepatic concentrations of the two endogenous ligands of CB_1 and CB_2 receptors, 2-AG and AEA (data not shown). Conversely, we observed a statistically significant decrease of the 2-acylglycerol derivative (i.e., 2-LG) and the ethanolamine derivative (i.e., LEA) of linoleic acid (LA), in *ob/ob* mice with respect to *db/db* mice. 13-HODE-G, which is a novel molecule derived from the 12-lipoxygenase-catalysed oxygenation of 2-LG [30], displayed also significantly lower levels in *ob/ob* compared to *db/db* mice. The levels of the omega-3 fatty acid, eicosapentaenoic acid (EPA), and its derivative 2-EPG were also decreased in *ob/ob* mice with respect to the diabetic group, although the latter difference did not reach statistical significance ($P = 0.072$). Accordingly, the levels of 15- and 18-HEPE, which are both EPA bioactive metabolites, were also significantly reduced in the *ob/ob* compared to *db/db* group. The 2-DPG, which derives from another omega-3 fatty acid, DPA, presented also a trend towards lower levels in *ob/ob* mice compared to *db/db* mice, whilst the amounts of the derivative of the omega-3 fatty acid DHA, 2-DHG, displayed an opposite and strongly significant increase in *ob/ob* with respect to *db/db* mice. However, no significant differences were observed in the concentration of

DPA and DHA between the two groups (data not shown). The hepatic levels of two main NAEs, OEA and PEA, were also significantly higher in *ob/ob* than *db/db* mice as were those of the 2-monoacylglycerol 2-OG. We also examined the hepatic concentration of non-eCBome mediators such as the prostaglandins, and found a significant increase of PGD_2 and PGE_2 levels in *ob/ob* with respect to *db/db* mice.

We then investigated if the changes found in the levels of the eCBome mediators were accompanied by modulation of the mRNA expression of their anabolic and catabolic enzymes or receptors (Figure 1B). Regarding receptors, there were statistically significant changes in the expression of *Pparg*, *Ptgfr* and *Trpv2*, which were augmented in the liver of *ob/ob* with respect to the *db/db* mice. Stronger differences in gene expression were observed at the level of eCBome-related metabolic enzymes. Specifically, there was a global significant increase, in *ob/ob* compared to *db/db* mice, of: 1) the transcript levels of NAE biosynthetic enzymes, i.e. *Abhd4*, *Gdpd1*, *Inpp5d* and *Napepld*, which could potentially explain the increase of hepatic PEA and OEA levels in the *ob/ob* group, and 2) the transcript levels of MAG catabolic enzymes *Ces1d* and *Mgll*, which might instead explain the lower levels of 2-LG and 2-EPG, but not 2-DHG, in these mice.

Altogether, these results highlight a different anti-inflammatory hepatic eCBome profile between *ob/ob* and *db/db* mice, which may partially explain the earlier onset of liver inflammation and impaired liver function observed in *ob/ob* mice as found in Suriano et al., [25].

3.2 Different eCBome profiles in the adipose tissues of ob/ob and db/db mice

Despite the lower inflammatory tone in the liver, *db/db* mice displayed elevated inflammation-related parameters in both subcutaneous and visceral adipose tissue (SAT and VAT) depots, with the SAT presenting the most pronounced inflammatory phenotype [25].

In this latter tissue (Figure 2A), we found no difference for the endocannabinoid 2-AG between the *ob/ob* and *db/db* mice (data not shown). However, the 2-acylglycerols 2-PG, 2-OG and 2-DHG, and the 2-LG 12-lipoxygenase metabolite, 13-HODE-G were all decreased in *db/db* with respect to *ob/ob* mice, while 2-LG presented only a trend towards a decrease. Regarding NAEs, there were no differences, whereas significantly higher levels of the omega-3 fatty acids EPA and DPA were present in the *db/db* compared to the *ob/ob* group. In the VAT (Figure 3A), despite clear trends, no statistically significant differences were observed for almost

all the molecules studied, the only exceptions being AEA and *N*-docosahexaenoylethanolamine (DHEA), the levels of which were significantly decreased in the *db/db* group.

Concerning the genes encoding eCBome-related receptors (Figure 2B and 3B), for SAT and VAT, respectively), *Cnr2*, *Pparg* and *Trpv2* were the only ones showing differential gene expression between the *ob/ob* and *db/db* groups. In particular, while in SAT the transcript levels of these receptors were significantly modified, with *Cnr2* and *Trpv2* showing an increased expression in *db/db* respect to *ob/ob* mice and *Pparg* having an opposite significant trend, in VAT the changes were in the same direction as SAT but statistically significant only for *Pparg* and *Trpv2*.

Regarding eCBome anabolic and catabolic enzymes, significant differences were found for the gene expression of 2-monoacylglycerol biosynthetic enzyme *Plcb1*, the lipoxygenase *Alox12* and the NAE anabolic enzyme *Gde1*. Specifically, if in SAT only the mRNA expression of *Plcb1* and *Alox12* displayed a significant decrease in the *db/db* group, in the VAT there was a statistically significant reduction also for *Gde1*. The decreased transcript levels of *Plcb1* in the SAT could explain the observed reduction of most 2-acylglycerols, although the decreased expression was stronger in the VAT, where we found no significant decrease in these mediators. Also, the decrease in the expression of SAT *Alox12* and of VAT *Gde1* in the *db/db* mice, might explain the reduction, in the *db/db* group, of SAT 13-HODE-G and of VAT NAEs levels, respectively. Other alterations remarked in both adipose tissue depots are shown in supplemental Table S4 and Table S5, for SAT and VAT, respectively.

The aforementioned results highlight an anti-inflammatory mediator profile that was more markedly modified in the SAT than in the VAT when comparing *ob/ob* and *db/db* mice, thus possibly explaining in part the more pronounced inflammatory phenotype in this tissue. Conversely, receptor and enzyme expression were similarly modified in the two adipose depots. Globally, these results seem to fit with the increase of the inflammation-related parameters in *db/db* with respect to *ob/ob* mice as observed in Suriano et al., [25].

3.3 Correlations between eCBome mediators and inflammation in the liver and the two adipose tissue depots

Given the different eCBome profiles observed in the liver and the two adipose tissue depots between *ob/ob* and the *db/db* mice, we explored correlations between previously obtained metabolic parameters in these three

different biological sites and published in Suriano et al., [25], and eCBome mediator tissue concentrations or metabolic enzyme and receptor mRNA expression levels. Analysis of the Pearson's rank correlation matrix confirmed the existence of potential links between certain eCBome-lipids and genes and several metabolic parameters. In details, starting from the liver, the matrix correlation showed that LA, 2-LG, and LEA were negatively correlated with liver weight, markers associated with a steatosis state (i.e., total lipid (TL) content, triglyceride (TG) and cholesterol (CHOL) content)), immune cell recruitment markers (i.e., *Itgax*, crown-like structures number (CLSn)), and a marker associated with a fibrosis state (*Tgfb1*), and a bile acid metabolism marker (i.e., *Abcb4*); EPA was positively correlated with a bile acid metabolism marker (*Slc27a5*); 15-HEPE was positively correlated with the LPS concentration; 2-DHG, and 2-OG were positively correlated with markers of steatosis (i.e., TL content), immune cell recruitment and inflammatory markers (i.e. *Ccl2*, *Itgax*, CLSn, *Cd14*, *Tlr2*), fibrosis markers (i.e., *Col1a1, Tgfb1*), and bile acid metabolism marker (i.e., *Slc51b*); PGE_2 was positively associated with immune cells recruitment markers (i.e., *Ccl2*, *Cd68*). In addition, most of the receptors and metabolic enzymes for the eCBome-mediators were positively correlated with the final body weight, final fat mass (FM), liver weight, steatosis (i.e., TL, TG and CHOL content), immune cell recruitment and inflammation markers (i.e., *Ccl2*, *Itgax*, *Cd68*, CLSn, *Cd14*, *Tlr4*, *Tlr2*, *Tlr5*, *Nlrp3*, *Tnf*, *Il1b*), fibrosis markers (i.e., *Col1a1*, *Tgfb1*), and bile acid metabolism markers (*Abcb4*, *Slc51b*); and negatively correlated with other bile acid metabolism markers (*Cyp27a1*, *Slc10a1*, *Oatp1b2*) (Figure 4).

Contrary to what we observed in the liver, we found that, in the SAT, 2-PG, 2-OG, 2-LG, and *Plcb1* were positively correlated with the inflammatory marker *Tlr5*; DPA was positively correlated with SAT weight, LPS concentration, and a marker of immune cell recruitment (i.e., *Ccl2*); similarly, *Cnr2* was positively correlated with another marker of immune cell recruitment (i.e., *Cd68*) (Figure 5A). On the other hand, in the VAT, *Cnr2* was positively correlated with final body weight, final FM, VAT weight, LPS concentration, immune cell recruitment and inflammatory markers (i.e., *Ccl2*, *Adgre1*, *Itgax*, *Cd68*, *Tlr4*, *Tlr2*, and *Il1b*); *Pparg* and *Gde1* were both negatively correlated with final body weight, final FM, VAT weight, LPS concentration, immune cell recruitment, and inflammation markers (i.e., *Adgre1*, *Itgax*, *Cd68*, and *Il1b*) (Figure 5B). Taken together, these observations highlight how eCBome signaling may be involved in modulating, or being modulated by, various metabolic and inflammatory pathways in three different biological sites, whose functions are closely related to obesity and associated metabolic disorders.

3.4 Correlations between eCBome mediators and gut microbiota taxa with emphasis on taxa involved in inflammation

Changes in the composition of the GM could partly underlie, or be caused by, alterations in eCBome signaling described above, thereby contributing both directly and indirectly to the different inflammatory tone described in the liver and the two adipose tissue depots. To this end, we investigated the existence of correlations between eCBome mediator tissue concentrations or metabolic enzyme and receptor mRNA expression levels and the relative abundance of bacterial taxa that were significantly, or tended to be, different between *ob/ob* and *db/db* mice. When exploring such correlations using Spearman's rank correlation matrix, we observed that several bacterial taxa belonging to the *Firmicutes* phylum were either positively or negatively correlated with the eCBome signaling. In details, *Clostridium_sensu_stricto*_1, was negatively correlated with hepatic concentrations of 2-LG, 13-HODE-G, and EPA, and positively correlated with PEA and PGD_2; *Dubosiella*, was positively correlated with PGD_2; *Lachnospiraceae*_UCG_006, was positively correlated with 15-HEPE; *Turicibacter*, was negatively correlated with EPA and positively correlated with PEA, PGE_2, and PGD_2. On the other hand, *Rikenellaceae*_RC9_gut.group, belonging to the *Bacteroidetes* phylum was negatively correlated with PEA and PGD_2; *Bacteroides*, belonging to the same phylum was negatively correlated with PGD_2 (Figure 6). We also found that *Clostridium_sensu_stricto*_1 was positively correlated with the SAT 13-HODE-G and *Pparg*, while *Turicibacter* was positively correlated with the SAT 2-DHG and 13-HODE-G (Figure 7A). The same bacterial taxa, as well as *Dubosiella*, were both positively correlated with the VAT level of *Plcb1* (Figure 7B). These correlative data suggest the existence of a direct or indirect cross-talk between eCBome signaling in the liver, SAT or VAT and the GM.

4. Discussion

In the present study, we aimed at exploring whether alterations, either at the transcription level or in term of tissue concentrations of molecules belonging to the eCBome, a complex signaling system whose dysregulation is associated with different pathological conditions (e.g., obesity, type 2 diabetes) [1, 13, 18, 31], could reflect the different inflammatory phenotypes that we previously observed in genetically obese (*ob/ob*) and diabetic (*db/db*) mice [25]. Although both mutant mice exhibit the same body weight and fat mass gain evolution over the course of the experiment, they develop distinctive inflammatory phenotypes, with the liver being more inflamed in *ob/ob* mice, and the adipose tissues being more inflamed in *db/db* mice. Seeking for a causal factor, the results we provide are unique since they represent a comprehensive investigation of how bioactive lipids as well as receptors and enzymes belonging to eCBome and related prostaglandin signaling may potentially sustain or counteract the tissue-dependent inflammatory state in mice having the same body weight but different glucose homeostasis. We identified the presence of a possible inflammation-related molecular profile, since some of the observed alterations were characteristic of all tissues showing the most pronounced inflammatory response, i.e.: 1) 2-LG and its 12-lipoxygenase metabolite 13-HODE-G [30] were present in reduced concentrations, and 2) *Trpv2* showed increased expression, in both the liver of *ob/ob* mice and the adipose tissue depots of *db/db* mice. While still little is known about the receptors of 13-HODE-G, the levels of the established targets for 2-LG, i.e. GPR119 and TRPV1 (activated by all saturated and polyunsaturated 2-MAGs [32]), were not modified in either liver and adipose tissues of obese and diabetic mice. Interestingly, GPR119 is also activated by: 1) 2-OG, whose levels were also reduced in the liver and SAT of *db/db* mice, and 2) LEA, a NAE whose levels were significantly decreased in the liver of *ob/ob* mice. Regarding the non-selective cation channel *Trpv2*, its expression in immune cells suggests a role in the immune response and inflammation [33, 34], and, in hepatomas, a stimulatory function on oxidative stress [35]. To date, the only eCBome mediators that have been shown to act as TRPV2 ligands are the unsaturated long chain NAEs, such as LEA, which were found to antagonize this channel [36]. Therefore, we hypothesize that the more pronounced inflammatory tone in the liver and adipose tissues of *ob/ob* and *db/db* mice, respectively, might be due in part to higher expression of *Trpv2* and, in the former case, to the lower levels of its endogenous

antagonist LEA. However, the contribution of TRPV2 to inflammation requires further investigations, and *in vitro* and *in vivo* experiments are needed to elucidate its role in the context of obesity.

In addition to those mentioned above, other tissue-specific inflammation-related changes were observed. We found significantly decreased levels of the omega-3 fatty acid EPA and its derivatives in *ob/ob* mice, characterized by inflammation-related hepatic injuries. It is known that n-3 PUFAs exert metabolic benefits, which may also result from the elevation of their corresponding NAEs and 2-MAGs [37], as well as other *N*-acylamides [38], which possess anti-inflammatory and anti-cancer actions and potential cardiometabolic and neuroprotective effects independent of cannabinoid receptors [39-42]. In agreement with this hypothesis, and with the reduced availability of EPA, we also remarked a decrease of the eCBome EPA derivative, 2-EPG, as well as of the bioactive metabolites 15- and 18-HEPE, in the liver of *ob/ob* mice. In contrast, we found increased levels of the DHA-derived 2-DHG in *ob/ob* mice, possibly as a compensatory mechanism to counteract the stronger hepatic inflammation observed in this group. Likewise, the increased levels of the two omega-3 PUFAs, EPA and DPA, in the more inflamed SAT of *db/db* mice led us to speculate about a possible negative feedback mechanism; however, the statistically significant reduced levels of the 2-DHG in this tissue were in agreement with a more pronounced inflammatory status. Regarding the VAT, we only observed reduced levels of the DHA-derived NAE, DHEA, which is known to exert anti-inflammatory effects in several inflammation models [40] as well as in LPS-induced inflammation in adipocytes [43], and might, therefore partly explain the higher inflammatory tone in the VAT of *db/db* mice. Accordingly, the expression levels of the nuclear receptor *Pparg*, which has been suggested to partially mediate, together with CB2, DHEA anti-inflammatory actions [43], were significantly decreased in the VAT of *db/db* mice.

Previous *in vitro* and *in vivo* studies have also described altered NAE and 2-MAG levels, together with an excessive activation/expression of CB1, in the liver and adipose tissue both at the cellular and tissue levels during obesity and diabetes, thereby leading to altered lipid and glucose metabolism as well as inflammation [3, 15, 44]. Consistently, *Cnr1* (encoding CB1)-KO mice are protected against diet-induced obesity [15]. However, in our study, no change in the expression of *Cnr1* was observed, nor in the levels of the endocannabinoid 2-AG in all the tissues considered, or of AEA hepatic and SAT levels, thus suggesting that CB1 activation by AEA or 2-AG, is not the main contributor to the stronger hepatic and adipose tissues

inflammation observed in *ob/ob* and *db/db* mice, respectively. In the VAT, in fact, the levels of AEA were significantly reduced in *db/db* compared to *ob/ob* mice, possibly in agreement with the decreased expression levels of the *Pparg*, which has been shown to be transcriptional activated by AEA in the micromolar concentration range [45, 46], to stimulate the differentiation of fibroblasts to adipocytes [45], and to exert anti-inflammatory effects [47].

Despite a more-pronounced liver inflammation, we observed increased hepatic levels of the two AEA congeners, OEA and PEA in *ob/ob* mice. Previous *in vitro* and *in vivo* studies have already described the anti-inflammatory, analgesic and neuroprotective effects exerted by OEA and PEA through PPAR□-dependent mechanisms [48-50]. Furthermore, administration of PEA induced significant improvement in a rat model of liver fibrosis, possibly by inhibiting the activation of hepatic stellate and Kupffer cells [51]. It is therefore possible that increased hepatic levels of OEA and PEA in *ob/ob* mice, together with higher hepatic expression of *Pparg*, are the result of compensatory mechanisms aimed at counteracting the hepatic inflammation and fibrosis observed in this model. A similar compensatory mechanism may have occurred in the SAT (and, in a non-statistically significant manner, in the VAT) of *db/db* mice through an increased expression of the eCB receptor, *Cnr2*, a well-characterized anti-inflammatory receptor, known to be upregulated in a plethora of inflammatory conditions [52, 53].

From a more mechanistic point of view, the observed increase in the hepatic levels of some NAEs may be due to the increased expression of *Napepld*, the main anabolic enzymes for NAEs, as well as of other anabolic enzymes (i.e., *Abhd4*, *Gdpd1*, *Inpp5d*, and *Gde1*), which may also partially contribute to NAE biosynthesis [54]. We recently discovered that *Napepld* is a key regulatory enzyme whose function may go beyond the synthesis of NAEs, since its hepatocyte-specific deletion in mice was associated also with a marked modification of various bioactive lipids involved in host homeostasis, such as the bile acids (BAs) [55]. On the other hand, Margheritis et al., [56] demonstrated that BAs (i.e., deoxycholic acid) in turn modulate NAPE-PLD activity. We can therefore not exclude that the increased expression of *Napepld* may also be due to cholic acid, a primary bile acid, whose hepatic concentration is increased in *ob/ob* mice [25]. To date, however, there are no studies describing the modulation of NAPE-PLD by cholic acid and further investigations are needed in this direction. That being said, increased hepatic *Napepld* expression may explain the higher OEA and PEA levels, but not the lower LEA concentrations, in the liver, thus indicating that NAE biosynthesis is regulated

by different enzymes as well as by precursor availability (which, in the case of LEA, was indeed reduced in *ob/ob* mice). Likewise, the higher hepatic expression levels of 2-MAG-hydrolysing enzymes, i.e. carboxylesterase 1D (*Ces1d*) and, particularly, *Mgll*, might explain the lower levels of 2-LG, but not the increase of 2-OG, in *ob/ob* mice. Instead, in the SAT, the generalized decrease in 2-MAGs (but not 2-AG) observed in *db/db* mice may have resulted from the decreased expression of *Plcb1*, encoding the enzyme catalyzing the rate-limiting reaction in 2-MAG biosynthesis. However, *Plcb1* was also down-regulated in the VAT, where 2-MAG levels were not different between *ob/ob* and *db/db* mice. Finally, reduced expression of the NAE-biosynthetic enzyme, *Gde1*, was observed only in the VAT and so were the reduced concentrations of AEA and DHEA, but not of other NAEs, whereas the observed decrease in the expression of *Alox12* may explain the reduction in the levels of 13-HODE-G in the SAT, but not the lack of changes in this metabolite found in the VAT.

An additional potential mechanism underlying metabolic disorder-associated inflammation may be represented by the increase of two pro-inflammatory eicosanoids, the prostaglandins PGE_2 and PGD_2 as well as of the expression of the prostaglandin $F_{2\alpha}$ receptor *Ptgfr* observed in the liver of *ob/ob* mice compared to *db/db* mice [57].

Looking for specific links between eCBome-signaling and the metabolic parameters measured in the three different biological sites, we carried out correlation analyses and observed that eCBome mediator or metabolic enzyme/receptor gene expression levels were either positively or negatively correlated with several metabolic parameters linked to steatosis, recruitment of immune cells, and inflammation. This suggests that this complex endogenous signaling system may affect the metabolic function of the respective tissues. In particular, we noticed that hepatic 15-HEPE, suggested to act as an anti-inflammatory bio-active lipid [58, 59], was positively correlated with LPS levels, which may reflect a negative feedback response of the *db/db* mice aimed at counteracting steatosis, inflammation, and fibrosis. Increased circulating levels of LPS, a condition known as metabolic endotoxemia, were previously associated with obesity, insulin resistance, hepatic lipid accumulation, liver and adipose tissue inflammation [60-62]. The levels of the TRPV2 antagonist, LEA, and of 2-LG, were negatively correlated with hepatic TG content, which in turn is directly related to hepatic inflammation, thus supporting the aforementioned potent protective role of these two eCBome mediators

against liver inflammation in *ob/ob* mice. Additionally, on the one hand, PGE_2 levels, *Ptgfr*, *Mgll*, and *Trpv2* gene expression, and, on the other hand, *Pparg*, *Napepld*, and *Gde1* gene expression, which, as discussed above, have been associated with inflammation and immune cell recruitment or protection against it, respectively, were positively correlated with immune and inflammatory markers, liver weight or TG content, thus strengthening their possible role in causing, or attempting to adapt to, the higher lipid accumulation and inflammatory tone in the liver of *ob/ob* mice. In the two adipose tissues, fewer correlations were observed between eCBome signaling and metabolic parameters, which could suggest that other factors, in addition to the altered eCBome, may be implicated in the modulation of the inflammatory tone observed in the SAT and VAT, particularly in *db/db* mice. Nevertheless, we did observe the expected positive correlation between *Cnr2* and the macrophage marker *Cd68* in the SAT as well as with other inflammatory markers in the VAT, and negative correlations between *Pparg* and *Gde1* and LPS and other inflammatory markers in this adipose tissue depot, thus substantiating some of the speculations made above regarding the role of these eCBome members in adipose tissue inflammation in *db/db* mice. *Pparg* was also negatively correlated with VAT weight, but this may reflect the positive correlation between the latter and LPS, which inhibits adipocyte differentiation, with subsequent adipocyte death, recruitment of immune cells and inflammation, which are all typical features of *db/db* mice [44, 63].

Among the factors contributing to both hepatic and adipose tissue inflammation in obesity, we have previously shown that the gut microbiota may act as a key modulator, notably through the LPS-eCB system regulatory loops, of the adipose tissue metabolism/function and general lipid homeostasis regulation in the liver [44]. The gut microbiota has indeed been proposed to regulate levels of endocannabinoids in the adipose tissue and the gut, and changes in its composition are sufficient to reduce peripheral eCB system tone in genetically induced and diet-induced models of obesity [5]. To provide indirect evidence that the gut microbiota plays a role in determining eCBome participation in the inflammatory phenotype of *ob/ob* mouse livers or *db/db* mouse adipose tissue, we analyzed the correlation between the eCBome members and the absolute abundance of certain fecal bacterial taxa that were different between the two mutant mice models [25]. Interestingly, some bacterial taxa were either positively or negatively correlated with certain eCBome-related molecules and receptors. Among them, *Clostridium_sensu_stricto*_1 deserves particular attention since its absolute quantity was significantly higher in *ob/ob* mice than in *db/db* mice and was positively correlated with either pro-

inflammatory (i.e., PGD2) or anti-inflammatory (i.e., PEA) hepatic bioactive lipids, and negatively correlated with other anti-inflammatory bioactive lipids (i.e., 2-LG, 13-HODE-G, and EPA). As a matter of fact, recent findings in humans and mice showed that this bacterial taxon was positively correlated with indicators of body weight and serum lipids [64], and with all non-alcoholic fatty-liver disease parameters [65]. In our present study, the same bacterial taxon was positively correlated with the levels of the putative anti-inflammatory lipid 13-HODE-G, and *Pparg* expression, measured in the SAT, suggesting a negative feedback response aiming at counteracting inflammation, whereas in the VAT *Clostridium_sensu_stricto*_1 was positively correlated with *Plcb1* expression.

Taken together, the results from our correlational analyses reinforce the hypothesis that the different profiles of eCBome signaling observed in the liver and adipose tissue depots of *ob/ob* and *db/db* mice may contribute to the respective inflammatory phenotypes in these tissues. However, more studies are needed to elucidate whether the identified eCBome-related molecules and their respective receptors and enzymes have a causal role in inflammation in these two genetically obese mice models. Indeed, the major limitation of this study consists in the lack of new *in vitro* experiments to elucidate the mechanisms of action of the eCBome members found to undergo differential changes in this study, and the reliance on previously published data on this aspect. Consequently, our correlation analyses do not imply causation and will require further studies.

In conclusion, the present study shows potential divergences in eCBome signaling between *ob/ob* and *db/db* mice that could be related to the etiology or consequences of the different inflammatory tone observed in the liver and the adipose tissue depot of these two mutant strains. The identification of such bioactive lipids and their related receptors and anabolic/catabolic enzymes may represent the basis of novel therapeutic approaches to tackle inflammation, which is a well-known common feature associated with obesity and diabetes. Besides, this work identified host-microbiome-eCBome interactions whose relevance in the context of obesity-related inflammation needs to be further assessed by means of mechanistic studies.

Data Availability

Data are showed within the manuscript and in the supplemental information files. For the correlation analysis between the eCBome signaling and the gut microbiota, we re-used the microbial data previously published in Suriano et al., [25]. The raw amplicon sequencing data are available in the European Nucleotide Archive (ENA) at EMBL-EBI under accession number PRJEB44809.

Declaration of interest

None.

Authors' Contributions:

Conceptualization: F.S., P.D.C. and V.D. Methodology: F.S., C.M., N.F., P.D.C., V.D. Correlation analysis: F.S. and C.D. Funding acquisition: P.D.C., V.D., C.S., N.F. Investigation: F.S., C.M., N.F., C.D., M.V.H., C.S. Supervision: P.D.C and V.D. Resources: P.D.C., N.M.D., C.S., N.F., V.D. Writing - Original Draft: F.S., C.M., P.D.C. and V.D. Writing - Review & Editing: all the authors. All authors have read and agreed to the published version of the manuscript.

Acknowledgments

We thank B. Es Saadi and A. Puel for their excellent technical assistance. P.D.C. is a senior research associate at FRS-FNRS (Fonds de la Recherche Scientifique), Belgium. C.M. was the recipient of a post-doctoral boursary from the Joint International Research Unit on Chemical and Biomolecular Studies on the Microbiome and its Impact on Metabolic Health and Nutrition (JIRU-MicroMeNu), which is funded by the Sentinelle Nord-Apogée Program of Université Laval, funded in turn by the Federal Tri-Agency of Canada. V.D. is the holder of the Canada Excellence Research Chair on the Gut Microbiome-Endocannabinoidome Axis in Metabolic Health (CERC-MEND) at Université Laval, funded by the Federal Tri-Agency of Canada. V.D. is the recipient of two Canada Foundation for Innovation grants (37392 and 37858).

References

[1] L. Cristino, T. Bisogno, V. Di Marzo. (2020). Cannabinoids and the expanded endocannabinoid system in neurological disorders. Nat Rev Neurol, 16(1), 9-29. doi:10.1038/s41582-019-0284-z

[2] V. Di Marzo, and Wang, J. ((eds) (2015)). The Endocannabinoidome: The World of Endocannabinoids and Related Mediators. USA:Academic Press Books-Elsevier.

[3] A. Veilleux, V. Di Marzo, C. Silvestri. (2019). The Expanded Endocannabinoid System/Endocannabinoidome as a Potential Target for Treating Diabetes Mellitus. Curr Diab Rep, 19(11), 117. doi:10.1007/s11892-019-1248-9

[4] V. Di Marzo. (2020). The endocannabinoidome as a substrate for noneuphoric phytocannabinoid action and gut microbiome dysfunction in neuropsychiatric disorders. Dialogues Clin Neurosci, 22(3), 259-269. doi:10.31887/DCNS.2020.22.3/vdimarzo

[5] P.D. Cani, H. Plovier, M. Van Hul, L. Geurts, N.M. Delzenne, C. Druart, A. Everard. (2016). Endocannabinoids--at the crossroads between the gut microbiota and host metabolism. Nat Rev Endocrinol, 12(3), 133-143. doi:10.1038/nrendo.2015.211

[6] V. Di Marzo. (2018). New approaches and challenges to targeting the endocannabinoid system. Nat Rev Drug Discov, 17(9), 623-639. doi:10.1038/nrd.2018.115

[7] C.J. Hillard. (2018). Circulating Endocannabinoids: From Whence Do They Come and Where are They Going? Neuropsychopharmacology, 43(1), 155-172. doi:10.1038/npp.2017.130

[8] I.F. Arturo, and Fabiana, P. (2020). Endocannabinoidome. In eLS, John Wiley & Sons, Ltd (Ed.). doi:https://doi.org/10.1002/9780470015902.a0028301

[9] F. Piscitelli, V. Di Marzo. (2012). "Redundancy" of endocannabinoid inactivation: new challenges and opportunities for pain control. ACS Chem Neurosci, 3(5), 356-363. doi:10.1021/cn300015x

[10] V. Di Marzo. (2008). Endocannabinoids: synthesis and degradation. Rev Physiol Biochem Pharmacol, 160, 1-24. doi:10.1007/112_0505

[11] S. Castonguay-Paradis, S. Lacroix, G. Rochefort, L. Parent, J. Perron, C. Martin, B. Lamarche, F. Raymond, N. Flamand, V. Di Marzo, A. Veilleux. (2020). Dietary fatty acid intake and gut microbiota determine circulating endocannabinoidome signaling beyond the effect of body fat. Sci Rep, 10(1), 15975. doi:10.1038/s41598-020-72861-3

[12] C. Silvestri, V. Di Marzo. (2013). The endocannabinoid system in energy homeostasis and the etiopathology of metabolic disorders. Cell Metab, 17(4), 475-490. doi:10.1016/j.cmet.2013.03.001

[13] V. Di Marzo, C. Silvestri. (2019). Lifestyle and Metabolic Syndrome: Contribution of the Endocannabinoidome. Nutrients, 11(8). doi:10.3390/nu11081956

[14] N. Forte, A.C. Fernandez-Rilo, L. Palomba, V. Di Marzo, L. Cristino. (2020). Obesity Affects the Microbiota-Gut-Brain Axis and the Regulation Thereof by Endocannabinoids and Related Mediators. Int J Mol Sci, 21(5). doi:10.3390/ijms21051554

[15] B. Gatta-Cherifi, D. Cota. (2016). New insights on the role of the endocannabinoid system in the regulation of energy balance. Int J Obes (Lond), 40(2), 210-219. doi:10.1038/ijo.2015.179

[16] J.D. O'Hare, E. Zielinski, B. Cheng, T. Scherer, C. Buettner. (2011). Central endocannabinoid signaling regulates hepatic glucose production and systemic lipolysis. Diabetes, 60(4), 1055-1062. doi:10.2337/db10-0962

[17] V. Purohit, R. Rapaka, D. Shurtleff. (2010). Role of cannabinoids in the development of fatty liver (steatosis). AAPS J, 12(2), 233-237. doi:10.1208/s12248-010-9178-0

[18] I. Bazwinsky-Wutschke, A. Zipprich, F. Dehghani. (2019). Endocannabinoid System in Hepatic Glucose Metabolism, Fatty Liver Disease, and Cirrhosis. Int J Mol Sci, 20(10). doi:10.3390/ijms20102516

[19] M.A. Karwad, D.G. Couch, E. Theophilidou, S. Sarmad, D.A. Barrett, M. Larvin, K.L. Wright, J.N. Lund, S.E. O'Sullivan. (2017). The role of CB1 in intestinal permeability and inflammation. FASEB J, 31(8), 3267-3277. doi:10.1096/fj.201601346R

[20] K. Kempf, J. Hector, T. Strate, B. Schwarzloh, B. Rose, C. Herder, S. Martin, P. Algenstaedt. (2007). Immune-mediated activation of the endocannabinoid system in visceral adipose tissue in obesity. Horm Metab Res, 39(8), 596-600. doi:10.1055/s-2007-984459

[21] M. Maccarrone, I. Bab, T. Biro, G.A. Cabral, S.K. Dey, V. Di Marzo, J.C. Konje, G. Kunos, R. Mechoulam, P. Pacher, K.A. Sharkey, A. Zimmer. (2015). Endocannabinoid signaling at the periphery: 50 years after THC. Trends Pharmacol Sci, 36(5), 277-296. doi:10.1016/j.tips.2015.02.008

[22] R. Witkamp. (2016). Fatty acids, endocannabinoids and inflammation. Eur J Pharmacol, 785, 96-107. doi:10.1016/j.ejphar.2015.08.051

[23] A. Nagappan, J. Shin, M.H. Jung. (2019). Role of Cannabinoid Receptor Type 1 in Insulin Resistance and Its Biological Implications. Int J Mol Sci, 20(9). doi:10.3390/ijms20092109

[24] A. Stasiulewicz, K. Znajdek, M. Grudzien, T. Pawinski, A.J.I. Sulkowska. (2020). A Guide to Targeting the Endocannabinoid System in Drug Design. Int J Mol Sci, 21(8). doi:10.3390/ijms21082778

[25] F. Suriano, et al. (2021). Novel insights into the genetically obese (ob/ob) and diabetic (db/db) mice: two sides of the same coin. Microbiome, In press.

[26] E.G. Bligh, W.J. Dyer. (1959). A rapid method of total lipid extraction and purification. Can J Biochem Physiol, 37(8), 911-917. doi:10.1139/o59-099

[27] A. Everard, H. Plovier, M. Rastelli, M. Van Hul, A. de Wouters d'Oplinter, L. Geurts, C. Druart, S. Robine, N.M. Delzenne, G.G. Muccioli, W.M. de Vos, S. Luquet, N. Flamand, V. Di Marzo, P.D. Cani. (2019). Intestinal epithelial N-acylphosphatidylethanolamine phospholipase D links dietary fat to metabolic adaptations in obesity and steatosis. Nat Commun, 10(1), 457. doi:10.1038/s41467-018-08051-7

[28] C. Depommier, N. Flamand, R. Pelicaen, D. Maiter, J.-P. Thissen, A. Loumaye, M.P. Hermans, A. Everard, N.M. Delzenne, V. Di Marzo, P.D. Cani. (2021). Linking the Endocannabinoidome with Specific Metabolic Parameters in an Overweight and Insulin-Resistant Population: From Multivariate Exploratory Analysis to Univariate Analysis and Construction of Predictive Models. Cells, 10(1), 71.

[29] F.A. Iannotti, V. Di Marzo. (2020). The gut microbiome, endocannabinoids and metabolic disorders. J Endocrinol. doi:10.1530/JOE-20-0444

[30] T.A. Archambault AS, Martin C, Dumais E, Rakotoarivelo V, Laviolette M, Silvestri C, Kostrzewa M, Ligresti A, Boulet LP, Di Marzo V, Flamand N. (2020). Human eosinophils and neutrophils biosynthesize novel 15-lipoxygenase metabolites from 1-linoleoyl-glycerol and N-linoleoyl-ethanolamine. J Immunol 204(suppl 1): 220.28-220.28.

[31] G. Gruden, F. Barutta, G. Kunos, P. Pacher. (2016). Role of the endocannabinoid system in diabetes and diabetic complications. Br J Pharmacol, 173(7), 1116-1127. doi:10.1111/bph.13226

[32] P.M. Zygmunt, A. Ermund, P. Movahed, D.A. Andersson, C. Simonsen, B.A. Jonsson, A. Blomgren, B. Birnir, S. Bevan, A. Eschalier, C. Mallet, A. Gomis, E.D. Hogestatt. (2013). Monoacylglycerols activate TRPV1--a link between phospholipase C and TRPV1. PLoS One, 8(12), e81618. doi:10.1371/journal.pone.0081618

[33] T.C. Fricke, F. Echtermeyer, J. Zielke, J. de la Roche, M.R. Filipovic, S. Claverol, C. Herzog, M. Tominaga, R.A. Pumroy, V.Y. Moiseenkova-Bell, P.M. Zygmunt, A. Leffler, M.J. Eberhardt. (2019). Oxidation of methionine residues activates the high-threshold heat-sensitive ion channel TRPV2. Proc Natl Acad Sci U S A, 116(48), 24359-24365. doi:10.1073/pnas.1904332116

[34] C.M. Issa, B.D. Hambly, Y. Wang, S. Maleki, W. Wang, J. Fei, S. Bao. (2014). TRPV2 in the development of experimental colitis. Scand J Immunol, 80(5), 307-312. doi:10.1111/sji.12206

[35] W. Ma, C. Li, S. Yin, J. Liu, C. Gao, Z. Lin, R. Huang, J. Huang, Z. Li. (2015). Novel role of TRPV2 in promoting the cytotoxicity of H2O2-mediated oxidative stress in human hepatoma cells. Free Radic Biol Med, 89, 1003-1013. doi:10.1016/j.freeradbiomed.2015.09.020

[36] A. Schiano Moriello, S. Lopez Chinarro, O. Novo Fernandez, J. Eras, P. Amodeo, R. Canela-Garayoa, R.M. Vitale, V. Di Marzo, L. De Petrocellis. (2018). Elongation of the Hydrophobic Chain as a Molecular Switch: Discovery of Capsaicin Derivatives and Endogenous Lipids as Potent Transient Receptor Potential Vanilloid Channel 2 Antagonists. J Med Chem, 61(18), 8255-8281. doi:10.1021/acs.jmedchem.8b00734

[37] C.E. Ramsden, D. Zamora, A. Makriyannis, J.T. Wood, J.D. Mann, K.R. Faurot, B.A. MacIntosh, S.F. Majchrzak-Hong, J.R. Gross, A.B. Courville, J.M. Davis, J.R. Hibbeln. (2015). Diet-induced changes in n-3- and n-6-derived endocannabinoids and reductions in headache pain and psychological distress. J Pain, 16(8), 707-716. doi:10.1016/j.jpain.2015.04.007

[38] K.C. Verhoeckx, T. Voortman, M.G. Balvers, H.F. Hendriks, M.W. H, R.F. Witkamp. (2011). Presence, formation and putative biological activities of N-acyl serotonins, a novel class of fatty-acid derived mediators, in the intestinal tract. Biochim Biophys Acta, 1811(10), 578-586. doi:10.1016/j.bbalip.2011.07.008

[39] A. Arshad, W.Y. Chung, W. Steward, M.S. Metcalfe, A.R. Dennison. (2013). Reduction in circulating pro-angiogenic and pro-inflammatory factors is related to improved outcomes in patients with advanced pancreatic cancer treated with gemcitabine and intravenous omega-3 fish oil. HPB (Oxford), 15(6), 428-432. doi:10.1111/hpb.12002

[40] J.E. Watson, J.S. Kim, A. Das. (2019). Emerging class of omega-3 fatty acid endocannabinoids & their derivatives. Prostaglandins Other Lipid Mediat, 143, 106337. doi:10.1016/j.prostaglandins.2019.106337

[41] C.L. Wainwright, L. Michel. (2013). Endocannabinoid system as a potential mechanism for n-3 long-chain polyunsaturated fatty acid mediated cardiovascular protection. Proc Nutr Soc, 72(4), 460-469. doi:10.1017/S0029665113003406

[42] J. Meijerink, M. Balvers, R. Witkamp. (2013). N-Acyl amines of docosahexaenoic acid and other n-3 polyunsatured fatty acids - from fishy endocannabinoids to potential leads. Br J Pharmacol, 169(4), 772-783. doi:10.1111/bph.12030

[43] M.G. Balvers, K.C. Verhoeckx, P. Plastina, H.M. Wortelboer, J. Meijerink, R.F. Witkamp. (2010). Docosahexaenoic acid and eicosapentaenoic acid are converted by 3T3-L1 adipocytes to N-acyl ethanolamines with anti-inflammatory properties. Biochim Biophys Acta, 1801(10), 1107-1114. doi:10.1016/j.bbalip.2010.06.006

[44] G.G. Muccioli, D. Naslain, F. Backhed, C.S. Reigstad, D.M. Lambert, N.M. Delzenne, P.D. Cani. (2010). The endocannabinoid system links gut microbiota to adipogenesis. Mol Syst Biol, 6, 392. doi:10.1038/msb.2010.46

[45] M. Bouaboula, S. Hilairet, J. Marchand, L. Fajas, G. Le Fur, P. Casellas. (2005). Anandamide induced PPARgamma transcriptional activation and 3T3-L1 preadipocyte differentiation. Eur J Pharmacol, 517(3), 174-181. doi:10.1016/j.ejphar.2005.05.032

[46] V. Gasperi, F. Fezza, N. Pasquariello, M. Bari, S. Oddi, A.F. Agro, M. Maccarrone. (2007). Endocannabinoids in adipocytes during differentiation and their role in glucose uptake. Cell Mol Life Sci, 64(2), 219-229. doi:10.1007/s00018-006-6445-4

[47] C.E. Rockwell, N.E. Kaminski. (2004). A cyclooxygenase metabolite of anandamide causes inhibition of interleukin-2 secretion in murine splenocytes. J Pharmacol Exp Ther, 311(2), 683-690. doi:10.1124/jpet.104.065524

[48] S.E. O'Sullivan. (2016). An update on PPAR activation by cannabinoids. Br J Pharmacol, 173(12), 1899-1910. doi:10.1111/bph.13497

[49] M. Alhouayek, G.G. Muccioli. (2014). Harnessing the anti-inflammatory potential of palmitoylethanolamide. Drug Discov Today, 19(10), 1632-1639. doi:10.1016/j.drudis.2014.06.007

[50] S. Petrosino, V. Di Marzo. (2017). The pharmacology of palmitoylethanolamide and first data on the therapeutic efficacy of some of its new formulations. Br J Pharmacol, 174(11), 1349-1365. doi:10.1111/bph.13580

[51] M. Ohara, S. Ohnishi, H. Hosono, K. Yamamoto, Q. Fu, O. Maehara, G. Suda, N. Sakamoto. (2018). Palmitoylethanolamide Ameliorates Carbon Tetrachloride-Induced Liver Fibrosis in Rats. Front Pharmacol, 9, 709. doi:10.3389/fphar.2018.00709

[52] J. Paloczi, Z.V. Varga, G. Hasko, P. Pacher. (2018). Neuroprotection in Oxidative Stress-Related Neurodegenerative Diseases: Role of Endocannabinoid System Modulation. Antioxid Redox Signal, 29(1), 75-108. doi:10.1089/ars.2017.7144

[53] C. Turcotte, M.R. Blanchet, M. Laviolette, N. Flamand. (2016). The CB2 receptor and its role as a regulator of inflammation. Cell Mol Life Sci, 73(23), 4449-4470. doi:10.1007/s00018-016-2300-4

[54] G.G. Muccioli. (2010). Endocannabinoid biosynthesis and inactivation, from simple to complex. Drug Discov Today, 15(11-12), 474-483. doi:10.1016/j.drudis.2010.03.007

[55] C. Lefort, M. Roumain, M. Van Hul, M. Rastelli, R. Manco, I. Leclercq, N.M. Delzenne, V.D. Marzo, N. Flamand, S. Luquet, C. Silvestri, G.G. Muccioli, P.D. Cani. (2020). Hepatic NAPE-PLD Is a Key Regulator of Liver Lipid Metabolism. Cells, 9(5), 1247.

[56] E. Margheritis, B. Castellani, P. Magotti, S. Peruzzi, E. Romeo, F. Natali, S. Mostarda, A. Gioiello, D. Piomelli, G. Garau. (2016). Bile Acid Recognition by NAPE-PLD. ACS Chem Biol, 11(10), 2908-2914. doi:10.1021/acschembio.6b00624

[57] E. Ricciotti, G.A. FitzGerald. (2011). Prostaglandins and inflammation. Arterioscler Thromb Vasc Biol, 31(5), 986-1000. doi:10.1161/ATVBAHA.110.207449

[58] C. Wang, W. Liu, L. Yao, X. Zhang, X. Zhang, C. Ye, H. Jiang, J. He, Y. Zhu, D. Ai. (2017). Hydroxyeicosapentaenoic acids and epoxyeicosatetraenoic acids attenuate early occurrence of nonalcoholic fatty liver disease. Br J Pharmacol, 174(14), 2358-2372. doi:10.1111/bph.13844

[59] N.D. Hung, M.R. Kim, D.E. Sok. (2011). Mechanisms for anti-inflammatory effects of 1-[15(S)-hydroxyeicosapentaenoyl] lysophosphatidylcholine, administered intraperitoneally, in zymosan A-induced peritonitis. Br J Pharmacol, 162(5), 1119-1135. doi:10.1111/j.1476-5381.2010.01117.x

[60] P.D. Cani, J. Amar, M.A. Iglesias, M. Poggi, C. Knauf, D. Bastelica, A.M. Neyrinck, F. Fava, K.M. Tuohy, C. Chabo, A. Waget, E. Delmee, B. Cousin, T. Sulpice, B. Chamontin, J. Ferrieres, J.F. Tanti, G.R. Gibson, L. Casteilla, N.M. Delzenne, M.C. Alessi, R. Burcelin. (2007). Metabolic endotoxemia initiates obesity and insulin resistance. Diabetes, 56(7), 1761-1772. doi:10.2337/db06-1491

[61] P.D. Cani, R. Bibiloni, C. Knauf, A. Waget, A.M. Neyrinck, N.M. Delzenne, R. Burcelin. (2008). Changes in gut microbiota control metabolic endotoxemia-induced inflammation in high-fat diet-induced obesity and diabetes in mice. Diabetes, 57(6), 1470-1481. doi:10.2337/db07-1403

[62] P. Brun, I. Castagliuolo, V. Di Leo, A. Buda, M. Pinzani, G. Palu, D. Martines. (2007). Increased intestinal permeability in obese mice: new evidence in the pathogenesis of nonalcoholic steatohepatitis. Am J Physiol Gastrointest Liver Physiol, 292(2), G518-525. doi:10.1152/ajpgi.00024.2006

[63] M. Zhao, X. Chen. (2015). Effect of lipopolysaccharides on adipogenic potential and premature senescence of adipocyte progenitors. Am J Physiol Endocrinol Metab, 309(4), E334-344. doi:10.1152/ajpendo.00601.2014

[64] Q. Zeng, D. Li, Y. He, Y. Li, Z. Yang, X. Zhao, Y. Liu, Y. Wang, J. Sun, X. Feng, F. Wang, J. Chen, Y. Zheng, Y. Yang, X. Sun, X. Xu, D. Wang, T. Kenney, Y. Jiang, H. Gu, Y. Li, K. Zhou, S. Li, W. Dai. (2019). Discrepant gut microbiota markers for the classification of obesity-related metabolic abnormalities. Sci Rep, 9(1), 13424. doi:10.1038/s41598-019-49462-w

[65] O. Rom, Y. Liu, Z. Liu, Y. Zhao, J. Wu, A. Ghrayeb, L. Villacorta, Y. Fan, L. Chang, L. Wang, C. Liu, D. Yang, J. Song, J.C. Rech, Y. Guo, H. Wang, G. Zhao, W. Liang, Y. Koike, H. Lu, T. Koike, T. Hayek, S. Pennathur, C. Xi, B. Wen, D. Sun, M.T. Garcia-Barrio, M. Aviram, E. Gottlieb, I. Mor, W. Liu, J. Zhang, Y.E. Chen. (2020). Glycine-based treatment ameliorates NAFLD by modulating fatty acid oxidation, glutathione synthesis, and the gut microbiome. Sci Transl Med, 12(572). doi:10.1126/scitranslmed.aaz2841

Figure legends

Figure 1: Different hepatic eCBome tone in *ob/ob* and *db/db* mice. (**a**) Concentrations of the eCBome-related mediators in the liver tissue (fmol/mg wet tissue weight) measured by HPLC-MS/MS. (**b**) mRNA expression of receptors and metabolic enzymes for 2-monoacylglycerols and *N*-acylethanolamines measured by qPCR-based TaqMan Open Array. Green: CT ob lean mice, red: *ob/ob* mice, blue CT db lean mice, and violet: *db/db* mice. Data are presented as the mean ± S.E.M of n=9-10. * $P \leq 0.05$, ** $P \leq 0.01$, *** $P \leq 0.005$, **** $P \leq 0.001$. For mRNA expression, relative units were calculated versus the mean of the CT ob mice values set at 1. Data were analyzed by one-way ANOVA followed by Tukey's post hoc test. Abbreviations: see supplemental Table S1 and Table S2.

Figure 2: Different eCBome tone in the subcutaneous adipose tissue of *ob/ob* and *db/db* mice. (**a**) Concentrations of the eCBome-related mediators in the subcutaneous adipose tissue (fmol/mg wet tissue weight) measured by HPLC-MS/MS. (**b**) mRNA expression of receptors and metabolic enzymes for 2-monoacylglycerols and *N*-acylethanolamines measured by qPCR-based TaqMan Open Array. Green: CT ob lean mice, red: *ob/ob* mice, blue CT db lean mice, and violet: *db/db* mice. Data are presented as the mean ± S.E.M of n=9-10. * $P \leq 0.05$, ** $P \leq 0.01$, **** $P \leq 0.001$. For mRNA expression, relative units were calculated versus the mean of the CT ob mice values set at 1. Data were analyzed by one-way ANOVA followed by Tukey's post hoc test. Abbreviations: see supplemental Table S1 and Table S2.

Figure 3: Different eCBome tone in the visceral adipose tissue of *ob/ob* and *db/db* mice. (**a**) Concentration of the eCBome-related mediators in the visceral adipose tissue (fmol/mg wet tissue weight) measured by HPLC-MS/MS. (**b**) mRNA expression of receptors and metabolic enzymes for 2-monoacylglycerols and *N*-acylethanolamines measured by qPCR-based TaqMan Open Array. Green: CT ob lean mice, red: *ob/ob* mice, blue CT db lean mice, and violet: *db/db* mice. Data are presented as the mean ± S.E.M of n=9-10. ** $P \leq 0.01$, *** $P \leq 0.005$, **** $P \leq 0.001$. For mRNA expression, relative units were calculated versus the mean of the CT ob mice values set at 1. Data were analyzed by one-way ANOVA followed by Tukey's post hoc test. Abbreviations: see supplemental Table S1 and Table S2.

Figure 4: Correlation plot between altered metabolic parameters and eCBome-related mediators and mRNAs measured in the liver. Correlation matrix showing Pearson correlations with Bonferroni's adjustment in the liver. Positive correlations are shown in blue and negative correlations in red. Color intensity and size of the circles are proportional to the correlation coefficients. "X" refers to the first data set, the metabolic parameters measured in the liver while "Y" refers to the second data set, eCBome-related mediators and mRNAs measured in the liver.

Figure 5: Correlation plot between altered metabolic parameters and the eCBome-related mediators and mRNAs measured in the two adipose tissue depots. (**a**) Correlation matrix showing Pearson correlations with Bonferroni's adjustment in the subcutaneous adipose tissue; (**b**) Correlation matrix showing Pearson correlations with Bonferroni's adjustment in the visceral adipose tissue. Positive correlations are displayed in blue and negative correlations in red. Color intensity and size of the circles are proportional to the correlation coefficients. "X" refers to the first data set, the metabolic parameters measured in the two respective adipose tissue depots while "Y" refers to the second data set, the eCBome-related mediators and mRNAs measured in the two respective adipose tissue depots.

Figure 6: Correlation plot between altered bacterial taxa and eCBome-related mediators and mRNAs measured in the liver tissue. Correlation matrix (Pearson with Bonferroni's adjustment); positive correlations are displayed in blue and negative correlations in red. Color intensity and size of the circles are proportional to the correlation coefficients. "X" refers to the first data set, the altered bacterial taxa while "Y" refers to the second data set, the eCBome-related mediators and mRNAs measured in the liver.

Figure 7: Correlation plot between altered bacterial taxa and the eCBome-related mediators and mRNAs measured in the two adipose tissue depots. (**a**) Subcutaneous adipose tissue; (**b**) Visceral adipose tissue. Correlation matrix (Pearson with Bonferroni's adjustment); positive correlations are displayed in blue and negative correlations in red. Color intensity and size of the circles are proportional to the correlation coefficients. "X" refers to the first data set, the altered bacterial taxa while "Y" refers to the second data set, the eCBome-related mediators and mRNAs measured in the two respective adipose tissue depots.

Legends to the supplemental information files

Supplemental Table S1: Abbreviations of endocannabinoids and endocannabinoid-like molecules measured in three different tissues (i.e., liver, subcutaneous and visceral adipose tissues).

Supplemental Table S2: List of the genes analyzed by qPCR based TaqMan Open Array in three different tissues (i.e., liver, subcutaneous and visceral adipose tissues), and their metabolic function.

Supplemental Table S3: mRNA relative expression levels of receptors and metabolic enzymes for 2-monoacylglycerols and *N*-acylethanolamines measured by qPCR-based TaqMan Open Array in the liver tissue of *ob/ob* and *db/db* mice, and their respective littermates. Data are presented as the mean ± S.E.M of n=9-10. * $P \leq 0.05$, ** $P \leq 0.01$, *** $P \leq 0.005$, **** $P \leq 0.001$. Values are expressed as relative units calculated versus the mean of the CT ob mice values set at 1, and analyzed by one-way ANOVA. Abbreviations: see supplemental Table S1 and Table S2.

Supplemental Table S4: mRNA relative expression levels of receptors and metabolic enzymes for 2-monoacylglycerols and *N*-acylethanolamines measured by qPCR-based TaqMan Open Array in the subcutaneous adipose tissue of *ob/ob* and *db/db* mice, and their respective littermates. Data are presented as the mean ± S.E.M of n=9-10. Values are expressed as relative units calculated versus the mean of the CT ob mice values set at 1, and analyzed by one-way ANOVA. Abbreviations: see supplemental Table S1 and Table S2.

Supplemental Table S5: mRNA relative expression levels of receptors and metabolic enzymes for 2-monoacylglycerols and *N*-acylethanolamines measured by qPCR-based TaqMan Open Array in the visceral adipose tissue of *ob/ob* and *db/db* mice, and their respective littermates. Data are presented as the mean ± S.E.M of n=9-10. * $P \leq 0.05$, *** $P \leq 0.005$. Values are expressed as relative units calculated versus the mean of the CT ob mice values set at 1, and analyzed by one-way ANOVA. Abbreviations: see supplemental Table S1 and Table S2.

Supplemental Table S6: List of the deuterated internal standards used for LC/MS-MS analyses

Fig. 1

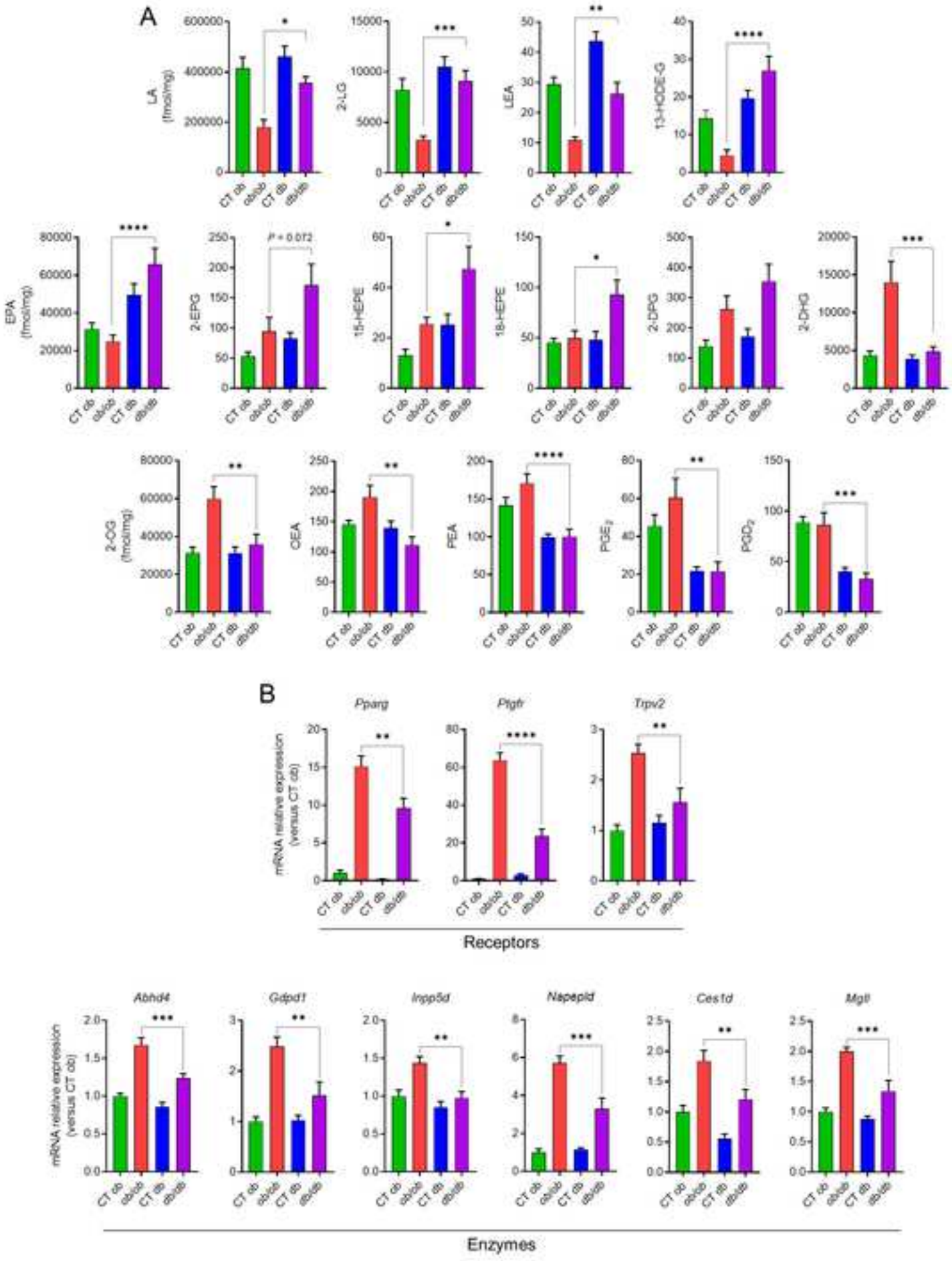

Fig. 2

Click here to access/download;Figure;Fig.2.tif

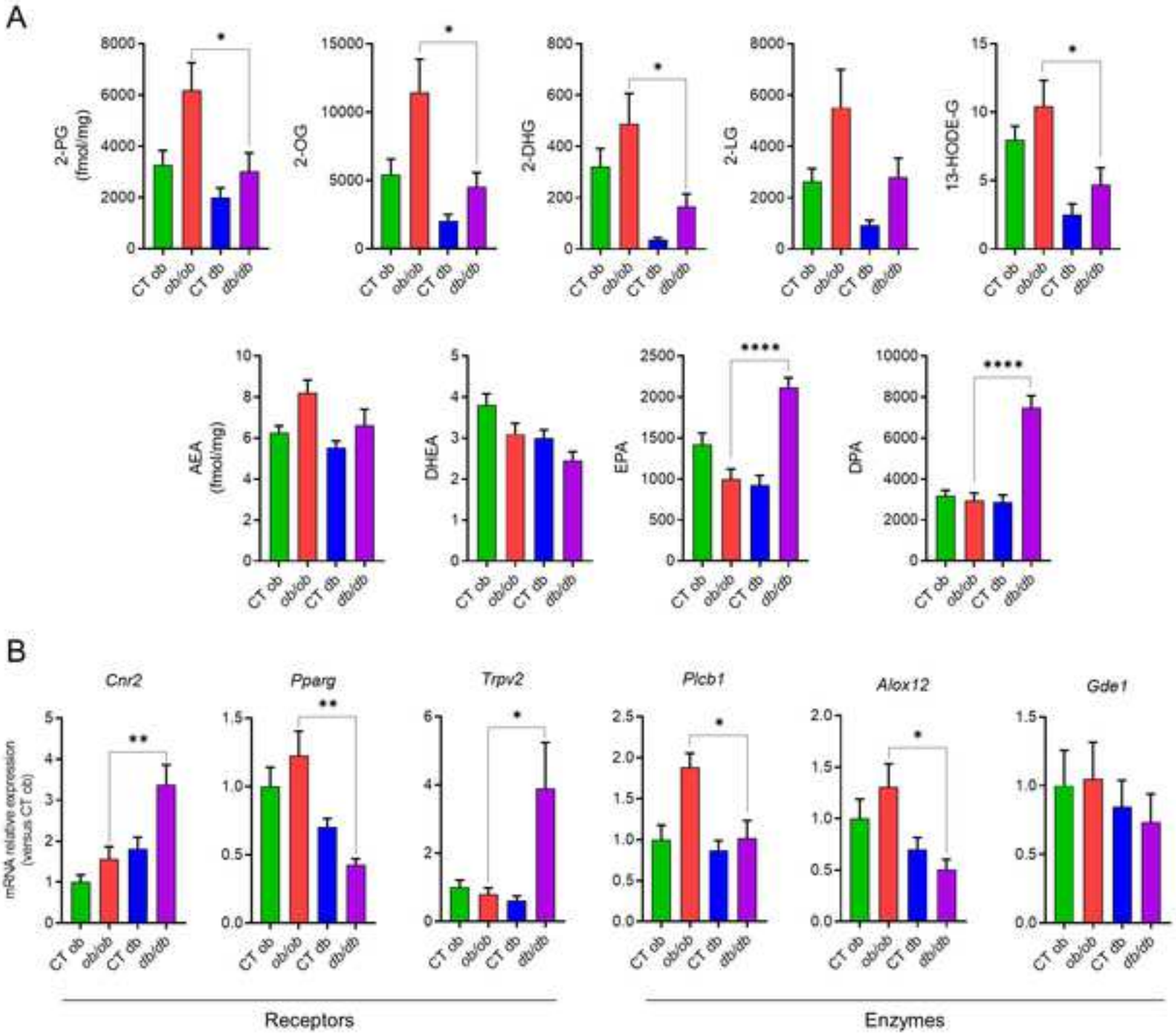

Fig. 3

Click here to access/download;Figure;Fig.3.tif

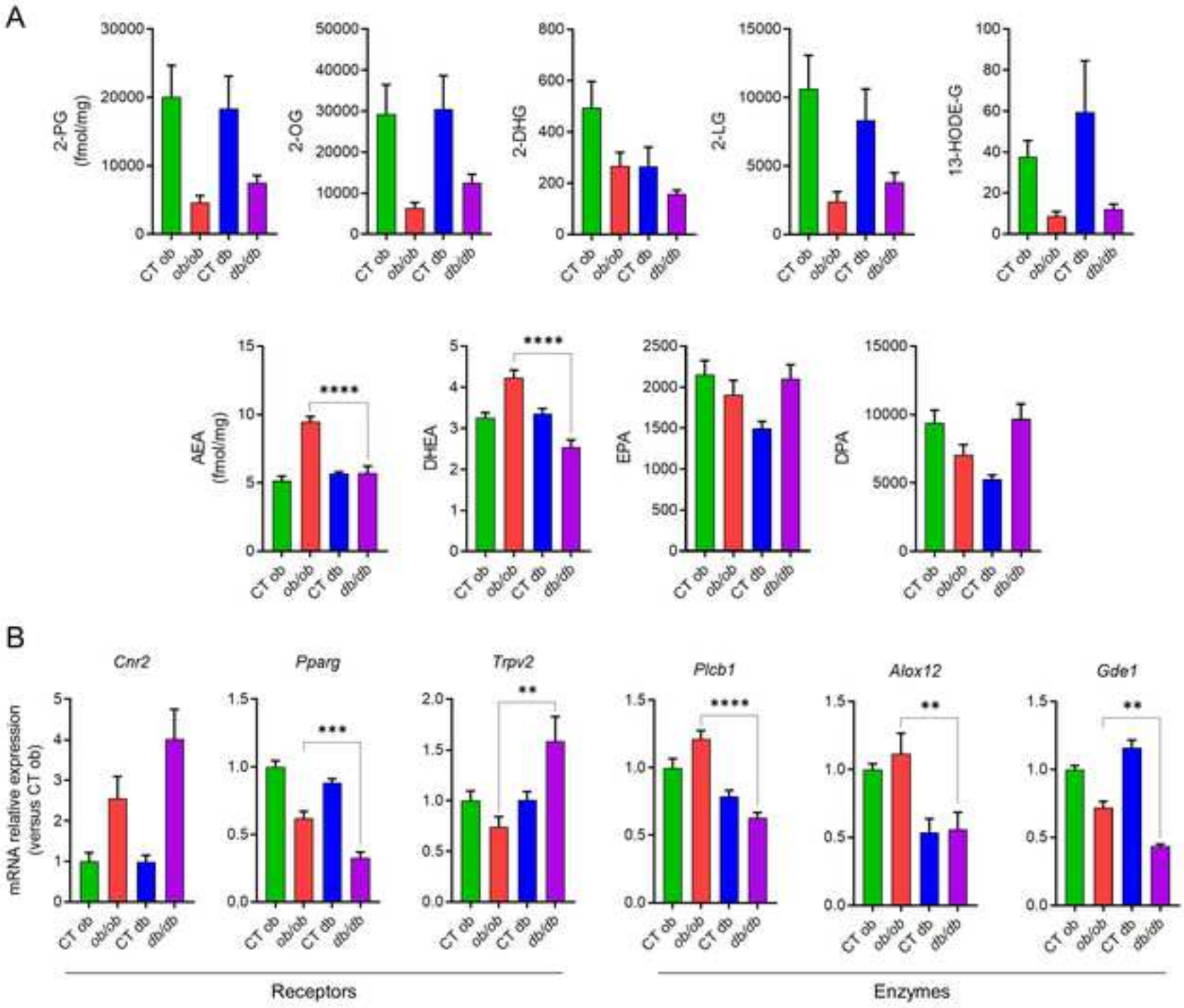

Fig. 4

Click here to access/download;Figure;Fig.4.tif

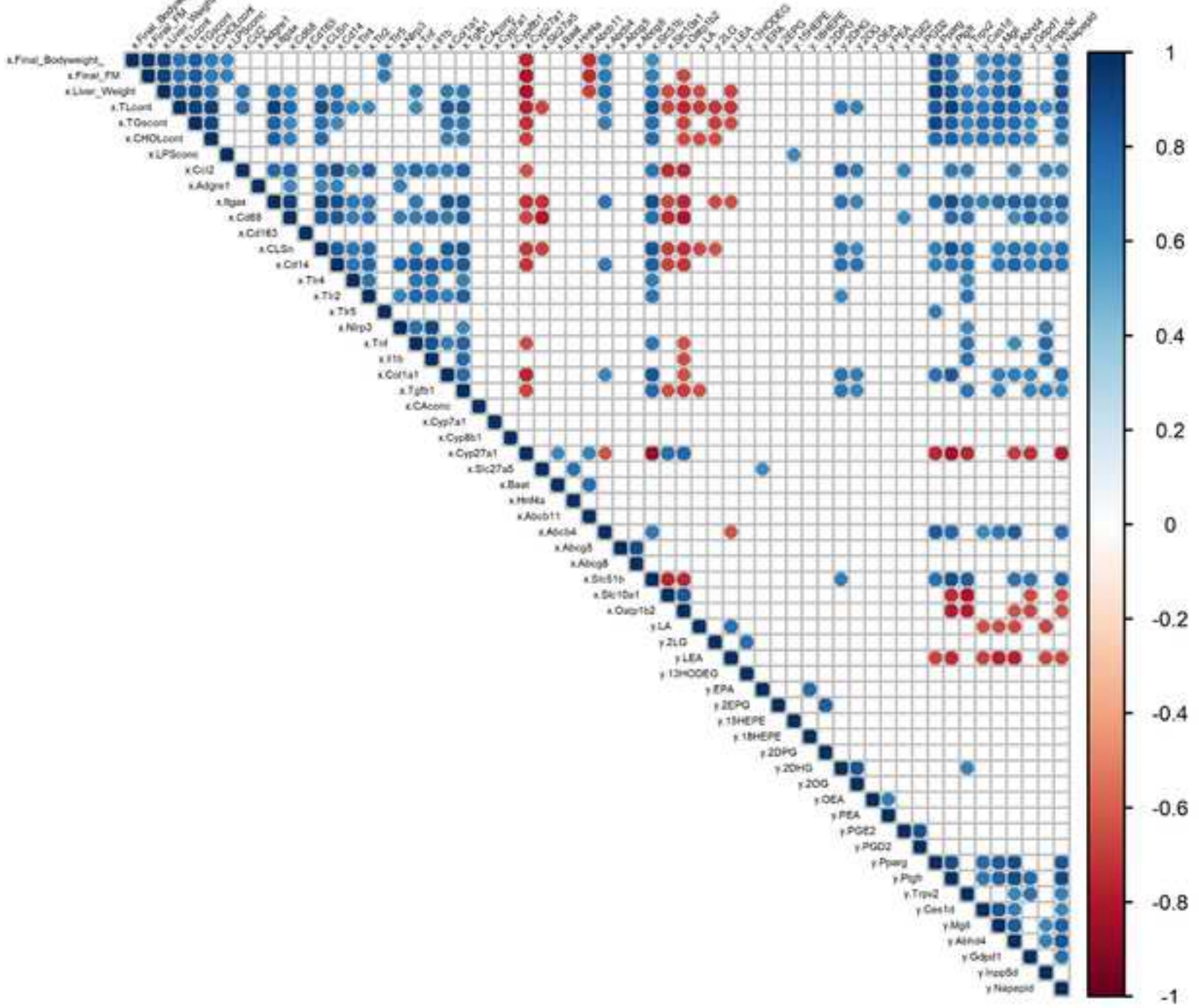

Fig. 5

Click here to access/download;Figure;Fig.5.tif

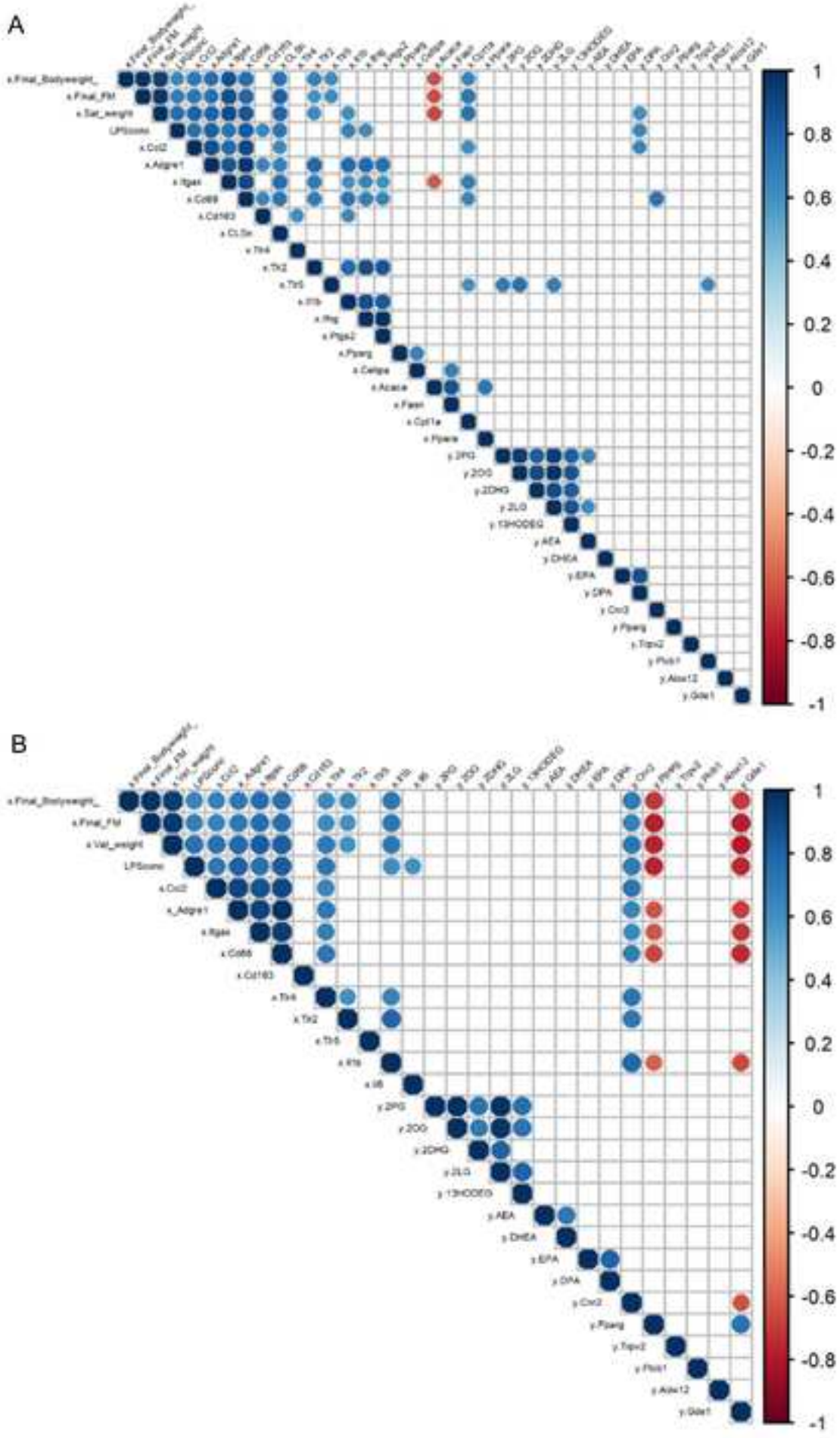

Fig. 6

Click here to access/download;Figure;Fig.6.tif

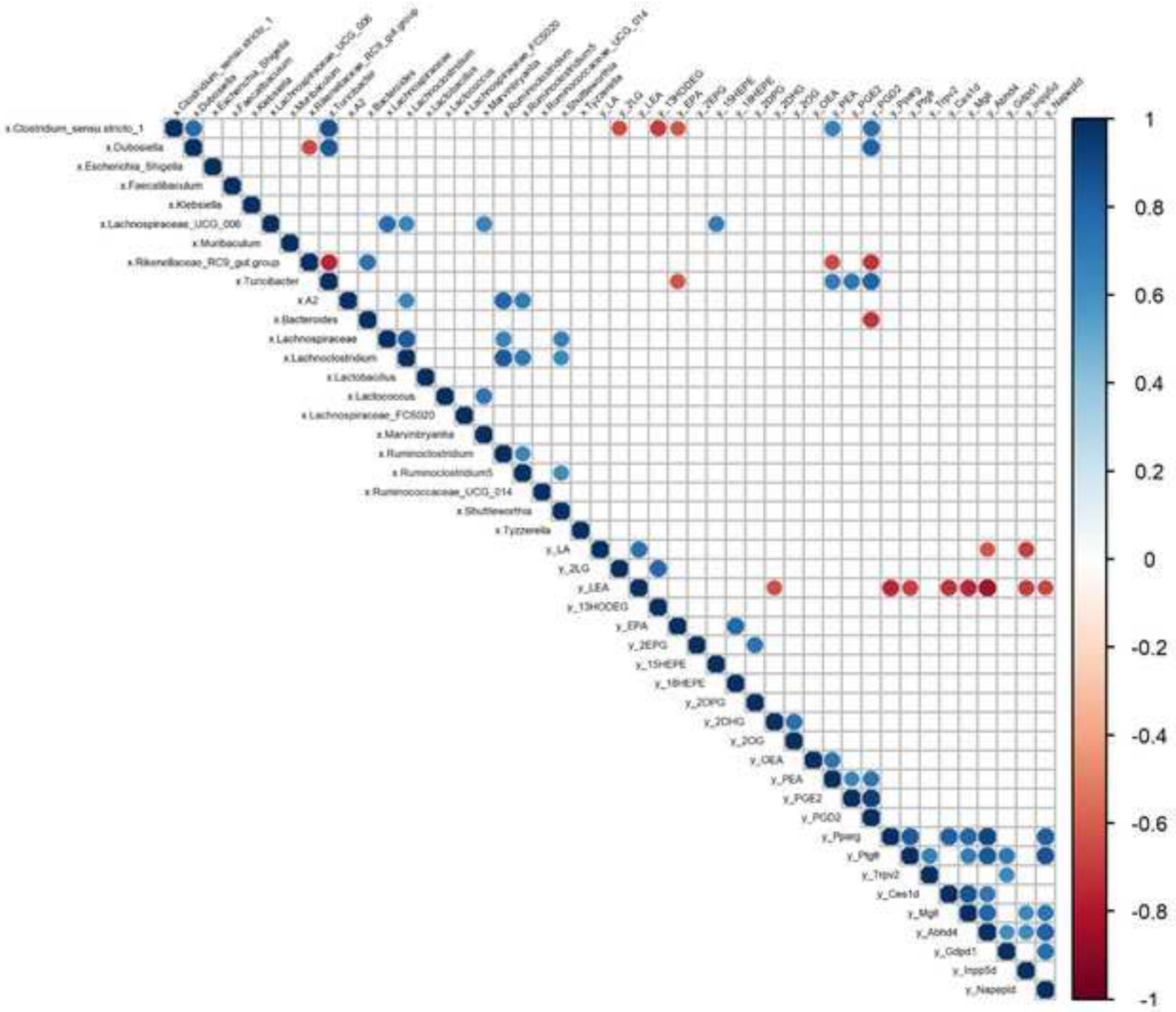

Fig. 7

Click here to access/download;Figure;Fig.7.tif

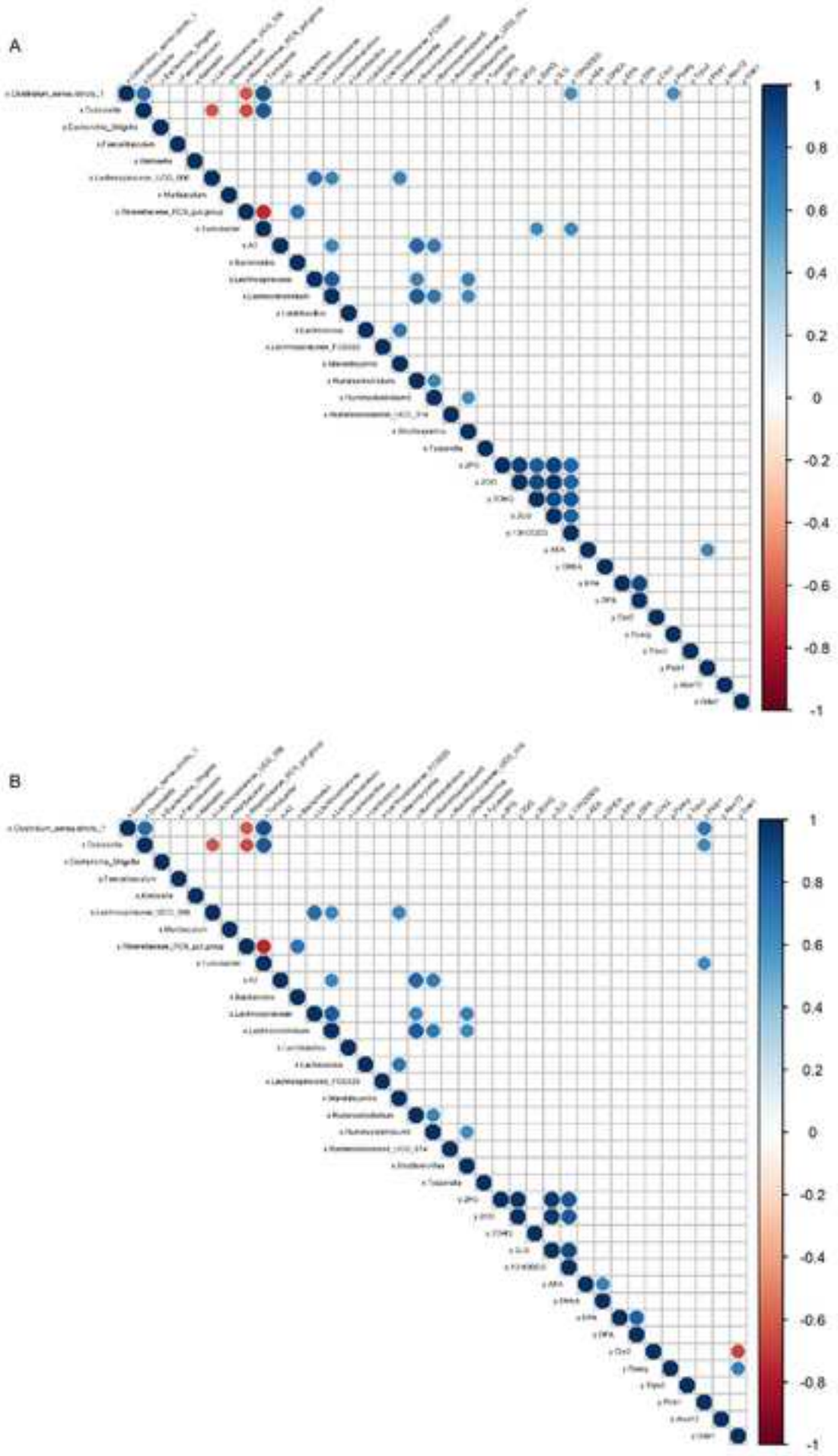

SUPPLEMENTAL INFORMATIONS

Supplemental. Table S1: Endocannabinoid and related lipid mediator abbreviations

Symbol	Endocannabinoids name
2-AG	1(3)- and 2-arachidonoyl-glycerol
AEA	*N*-arachidonoyl-ethanolamine
DHEA	*N*-docosahexanoyl-ethanolamine
2-DHG	1(3)- and 2-docosahexaenoyl-glycerol
DPA	docosapentaenoic acid (n-3)
2-DPG	1(3)- and 2-docospentaenoyl-glycerol (n-3)
EPEA	*N*-eicosapentanoyl-ethanolamine
EPA	eicosapentaenoic acid
2-EPG	2-eicosapentaenoyl-glycerol
15-HEPE	15-hydroxyeicosapentaenoic acid
18-HEPE	18-hydroxyeicosapentaenoic acid
13-HODE-G	13-Hydroxyoctadecadienoyl-glycerol
LA	Linoleic acid
LEA	*N*-linoleoyl-ethanolamine
2-LG	1(3)- and 2-linoleoyl-glycerol
SEA	*N*-stearoyl-ethanolamine
OEA	*N*-oleoyl-ethanolamine
2-OG	1(3)- and 2-oleoyl-glycerol
PEA	*N*-palmitoyl-ethanolamine
2-PG	2-palmitoyl-glycerol
PGD_2	Prostaglandin D_2
PGE_2	Prostaglandin E_2

Supplemental. Table S2: List of the genes analyzed by qPCR based TaqMan Open Array and their function

Gene symbol	Gene name	Function
Cacna1b	calcium channel, voltage-dependent, T type, alpha 1B subunit	receptor
Cacna1h	calcium channel, voltage-dependent, T type, alpha 1H subunit	receptor
Cnr1	cannabinoid receptor 1	receptor
Cnr2	cannabinoid receptor 2	receptor
Gpr119	G protein-coupled receptor 119	receptor
Gpr18	G protein-coupled receptor 18	receptor
Gpr55	G protein-coupled receptor 55	receptor
Ppara	peroxisome proliferator activated receptor alpha	receptor
Pparg	peroxisome proliferator activated receptor gamma	receptor
Ptgfr	prostaglandin F receptor	receptor
Trpv1	transient receptor potential cation channel, subfamily V, member 1	ligand-activated channel
Trpv2	transient receptor potential cation channel, subfamily V, member 2	ligand-activated channel
Trpv4	transient receptor potential cation channel, subfamily V, member 4	ligand-activated channel
Abhd4	abhydrolase domain containing 4	anabolic enzyme for NAEs
Akr1b3	aldo-keto reductase family 1, member B3 (aldose reductase)	anabolic enzyme for prostamides, catabolic enzyme for AEA and 2-AG
Fam213b	family with sequence similarity 213, member B	anabolic enzyme for prostamides, catabolic enzyme for AEA and 2-AG
Gde1	glycerophosphodiester phosphodiesterase 1	anabolic enzyme for NAEs
Gdpd1	glycerophosphodiester phosphodiesterase domain containing 1	anabolic enzyme for NAEs
Hrasls5	HRAS-like suppressor family, member 5	anabolic enzyme for NAEs
Inpp5d	inositol polyphosphate-5-phosphatase D	anabolic enzyme for NAEs
Napepld	N-acyl phosphatidylethanolamine-specific phospholipase D-like enzyme	anabolic enzyme for NAEs
Pla2g5	phospholipase A2, group V	AA-releasing enzyme possibly involved in phospholipid remodeling and hence biosynthesis of eCB precursors
Ptgs2	prostaglandin-endoperoxide synthase 2	anabolic enzyme for prostamides, catabolic enzyme for AEA and 2-AG
Ptpn22	protein tyrosine phosphatase, non-receptor type 22 (lymphoid)	anabolic enzyme for AEA
Ptges	prostaglandin E synthase	anabolic enzyme for prostamides, catabolic enzyme for AEA and 2-AG
Comt	catechol-O-methyltransferase	catabolic enzyme for *N*-acyl-dopamines
Faah	fatty acid amide hydrolase	catabolic enzyme for NAEs, primary fatty acid amides, *N*-acyl-taurines and *N*-acyl-glycines
Naaa	N-acylethanolamine acid amidase	catabolic enzyme for saturated NAEs
Pam	peptidylglycine alpha-amidating monooxygenase	anabolic enzyme for primary fatty acid amides, catabolic enzyme for *N*-acyl-glycines
Dagla	diacylglycerol lipase, alpha	anabolic enzyme for 2-acylglycerols

Daglb	diacylglycerol lipase, beta	anabolic enzyme for 2-acylglycerols
Dgke	diacylglycerol kinase, epsilon	anabolic/catabolic enzyme for 2-acylglycerols
Enpp2	ectonucleotide pyrophosphatase/phosphodiesterase 2	autotaxin- a LysoPLD: produces LPA.
Pla1a	phospholipase A1 member A	anabolic enzyme for 2-acylglycerols
Plcb1	phospholipase C, beta 1	anabolic enzyme for 2-acylglycerols
Abhd12	abhydrolase domain containing 12	catabolic enzyme for monocylglycerols
Abhd16a	abhydrolase domain containing 16	catabolic enzyme for monocylglycerols
Abhd6	abhydrolase domain containing 6	catabolic enzyme for monocylglycerols
Agk	acylglycerol kinase	catabolic enzyme for monocylglycerols
Alox12	arachidonate 12-lipoxygenase	catabolic enzyme for AEA and 2-AG
Alox15	arachidonate 15-lipoxygenase	catabolic enzyme for AEA and 2-AG
Ces1d	carboxylesterase 1D	catabolic enzyme for monoacylglycerols
Ces2h	carboxylesterase 2H	catabolic enzyme for monoacylglycerols
Mgll (Magl)	monoglyceride lipase	catabolic enzyme for monoacylglycerols
Mogat1	monoacylglycerol O-acyltransferase 1	catabolic enzyme for monoacylglycerols
Ppt1	palmitoyl-protein thioesterase 1	catabolic enzyme for 2-AG
Gapdh	glyceraldehyde-3-phosphate dehydrogenase	reference gene
Hprt	hypoxanthine guanine phosphoribosyl transferase	reference gene
Rps13	ribosomal protein S13	reference gene
Tbp	TATA box binding protein	reference gene

Supplemental. Table S3: List of the genes whose mRNA expression was detected in the liver by qPCR-based TaqMan Open Array

Gene symbol	*ob/ob*			CT db			*db/db*		
Cnr1	0.97	±	0.14	0.87	±	0.16	1.05	±	0.20
Gpr119	1.92	±	0.41	1.55	±	0.42	1.27	±	0.15
Gpr18	0.99	±	0.11	0.57	±	0.04	0.90	±	0.20
Gpr55	0.94	±	0.19	0.77	±	0.18	0.89	±	0.14
Ppara	1.03	±	0.08	0.90	±	0.05	1.12	±	0.08
Trpv4	1.78	±	0.28	1.63	±	0.19	2.46	±	0.27
Akr1b3	1.08	±	0.10	1.23	±	0.07	0.89	±	0.10
Fam213b	1.72	±	0.13	0.97	±	0.08	1.71	±	0.19
Gde1	1.55	±	0.12	0.91	±	0.09	1.72	±	0.12
Ptpn22	1.53 ***	±	0.11	0.76	±	0.06	0.81	±	0.14
Ptges	2.82	±	0.35	1.69	±	0.30	2.08	±	0.37
Comt	1.03	±	0.03	1.03	±	0.05	0.85	±	0.04
Faah	0.81	±	0.06	0.79	±	0.05	0.92	±	0.09
Naaa	1.42	±	0.09	1.04	±	0.08	1.14	±	0.05
Pam	2.00 *	±	0.19	0.85	±	0.08	1.36	±	0.13
Daglb	0.93	±	0.07	1.14	±	0.06	1.02	±	0.06
Dgke	1.87 ****	±	0.10	1.38	±	0.17	0.83	±	0.16
Enpp2	0.95	±	0.04	1.47	±	0.16	0.66	±	0.11
Pla1a	0.60 *	±	0.03	1.15	±	0.08	0.86	±	0.06
Plcb1	0.94	±	0.04	0.80	±	0.05	0.85	±	0.04
Abhd12	1.17	±	0.07	1.09	±	0.10	1.21	±	0.04
Abhd16a	1.59	±	0.08	1.05	±	0.14	1.27	±	0.04
Abhd6	2.44	±	0.18	1.00	±	0.08	2.15	±	0.28
Agk	1.49	±	0.04	1.20	±	0.08	1.40	±	0.07
Alox12	1.40 **	±	0.17	0.45	±	0.08	0.70	±	0.12
Alox15	2.89	±	1.30	2.38	±	0.45	9.30	±	2.95
Ces2h	1.04 ***	±	0.08	2.90	±	0.32	2.53	±	0.32
Mogat1	57.20	±	5.21	0.39	±	0.03	44.60	±	6.91
Ppt1	1.89 **	±	0.07	1.47	±	0.07	2.23	±	0.03

Supplemental. Table S4: List of the genes whose mRNA expression was detected in the subcutaneous adipose tissue by qPCR-based TaqMan Open Array

Gene symbol	***ob/ob***			**CT db**			***db/db***		
Cnr1	0.70	±	0.10	0.84	±	0.14	1.14	±	0.25
Gpr119	3.03	±	0.53	1.96	±	0.24	4.51	±	1.07
Gpr18	0.89	±	0.20	0.69	±	0.16	0.43	±	0.08
Gpr55	1.73	±	0.34	0.89	±	0.18	1.62	±	0.43
Ppara	0.37	±	0.13	1.03	±	0.30	0.42	±	0.17
Ptgfr	1.06	±	0.19	0.60	±	0.06	0.89	±	0.28
Trpv1	0.74	±	0.12	0.86	±	0.20	0.53	±	0.11
Abhd4	1.03	±	0.12	0.97	±	0.10	1.07	±	0.26
Akr1b3	1.14	±	0.26	1.16	±	0.23	0.95	±	0.21
Fam213b	1.43	±	0.41	0.72	±	0.16	0.87	±	0.29
Gdpd1	1.38	±	0.25	0.63	±	0.14	2.25	±	0.43
Hrasls5	0.30	±	0.07	0.48	±	0.12	0.43	±	0.14
Inpp5d	1.24	±	0.40	1.05	±	0.23	2.92	±	1.11
Napepld	1.23	±	0.51	0.87	±	0.22	1.39	±	0.57
Pla2g5	1.64	±	0.37	0.93	±	0.27	1.54	±	0.40
Ptpn22	1.82	±	0.16	1.00	±	0.08	2.00	±	0.26
Ptges	0.54	±	0.26	1.26	±	0.45	0.51	±	0.20
Comt	1.57	±	0.43	1.64	±	0.43	1.13	±	0.34
Naaa	1.09	±	0.27	1.00	±	0.20	0.89	±	0.18
Pam	7.66	±	1.76	1.13	±	0.22	5.63	±	1.63
Daglb	1.64	±	0.41	1.22	±	0.26	3.49	±	1.16
Dgke	0.70	±	0.09	0.64	±	0.12	0.63	±	0.11
Enpp2	1.79	±	0.46	0.88	±	0.13	2.33	±	0.57
Pla1a	0.94	±	0.25	0.84	±	0.21	0.58	±	0.16
Abhd12	1.63	±	0.46	0.92	±	0.20	2.12	±	0.40
Abhd16a	0.94	±	0.43	1.06	±	0.37	1.21	±	0.57
Abhd6	0.97	±	0.23	0.87	±	0.21	0.97	±	0.24
Agk	1.16	±	0.05	1.06	±	0.10	1.08	±	0.08
Ces1d	0.33	±	0.06	0.82	±	0.12	0.28	±	0.07
Mgll (Magl)	0.96	±	0.37	1.00	±	0.25	1.73	±	0.61
Mogat1	0.22	±	0.02	0.67	±	0.08	0.08	±	0.02
Ppt1	1.21	±	0.10	1.19	±	0.05	1.49	±	0.15

Supplemental. Table S5: List of the genes whose mRNA expression was detected in the visceral adipose tissue by qPCR-based TaqMan Open Array

Gene symbol	*ob/ob*			CT db			*db/db*		
Cacna1b	0.65	±	0.08	0.66	±	0.09	0.41	±	0.06
Cacna1h	0.38	±	0.09	0.58	±	0.10	0.13	±	0.02
Cnr1	0.74	±	0.09	0.88	±	0.10	0.77	±	0.09
Gpr119	1.97	±	0.54	0.88	±	0.14	1.45	±	0.46
Gpr18	1.18	±	0.18	0.88	±	0.12	1.11	±	0.26
Gpr55	2.87	±	0.81	1.18	±	0.14	1.88	±	0.46
Ppara	0.47	±	0.04	1.95	±	0.17	0.57	±	0.07
Ptgfr	0.65	±	0.08	0.47	±	0.05	0.26	±	0.03
Trpv1	0.79	±	0.13	0.76	±	0.12	0.52	±	0.06
Trpv4	0.94	±	0.14	1.14	±	0.10	1.32	±	0.21
Abhd4	0.74	±	0.08	0.92	±	0.05	0.67	±	0.03
Akr1b3	1.00 *	±	0.04	1.21	±	0.03	0.80	±	0.04
Fam213b	1.31 ***	±	0.04	0.73	±	0.04	0.80	±	0.11
Gdpd1	1.35	±	0.27	0.80	±	0.10	1.20	±	0.10
Hrasls5	1.00	±	0.08	1.11	±	0.06	1.12	±	0.06
Inpp5d	1.60	±	0.22	0.96	±	0.10	2.06	±	0.29
Napepld	0.72	±	0.08	1.20	±	0.08	0.76	±	0.11
Pla2g5	0.61	±	0.11	0.88	±	0.13	0.81	±	0.15
Ptgs2	0.68	±	0.17	0.83	±	0.15	0.37	±	0.04
Ptpn22	2.00	±	0.23	0.87	±	0.11	1.87	±	0.25
Ptges	0.75	±	0.06	1.26	±	0.09	0.50	±	0.08
Comt	0.77	±	0.06	1.45	±	0.10	0.58	±	0.10
Faah	0.52	±	0.05	0.58	±	0.09	0.43	±	0.07
Naaa	0.63	±	0.07	0.82	±	0.04	0.69	±	0.07
Pam	1.82	±	0.19	0.82	±	0.07	1.34	±	0.14
Dagla	1.21	±	0.29	1.11	±	0.23	0.87	±	0.14
Daglb	1.20	±	0.13	0.97	±	0.05	1.38	±	0.18
Dgke	0.79	±	0.07	0.88	±	0.08	0.52	±	0.08
Enpp2	0.76	±	0.10	1.02	±	0.07	0.96	±	0.10
Pla1a	0.95	±	0.12	0.91	±	0.05	0.82	±	0.10
Abhd12	1.33	±	0.09	1.11	±	0.07	1.33	±	0.11
Abhd16a	0.81	±	0.09	0.94	±	0.12	0.85	±	0.11
Abhd6	0.79	±	0.10	1.01	±	0.03	0.57	±	0.07
Agk	0.98	±	0.04	0.97	±	0.06	0.84	±	0.04
Alox15	1.08 *	±	0.19	3.06	±	0.28	3.33	±	0.98
Ces1d	0.28	±	0.02	0.91	±	0.05	0.32	±	0.06
Mgll (Magl)	0.80	±	0.05	1.23	±	0.06	0.95	±	0.08
Mogat1	0.30	±	0.02	0.99	±	0.05	0.17	±	0.03
Ppt1	0.91	±	0.09	1.50	±	0.08	1.15	±	0.07

Supplemental. Table S6: List of the deuterated internal standards used for LC/MS-MS analyses

Lipid mediators symbol	**Lipid mediators name**
2-AG	1-AG-d5
AA	AA-d8
AEA	AEA-d4
***N*-Arachidonoyl-Glycine**	*N*-Arachidonoyl Glycine-d8
***N*-Arachidonoyl-Serotonin**	*N*-Oleoyl-serotonin-d17
DHA	DHA-d5
DHEA	DHEA-d4
DPA	DPA-d5
2-DPG (n-3)	1-DPG-d5
EPA	EPA-d5
2-EPG	1-EPG-d5
EPEA	EPEA-d4
LEA	LEA-d4
2-LG	1-LG-d5
***N*-Oleoyl-Serine**	*N*-Oleoyl-Serine-d2
2-OG	1-AG-d5
***N*-Oleoyl-Serotonin**	*N*-Oleoyl-serotonin-d17
OEA	OEA-d4
PEA	PEA-d4
2-PG	1-AG-d5
PGE_2	PGE_2-d4
PGE_2-EA	PGE_2-EA-d4
PGE_2-G	PGE_2-G-d5
$PGF_{2\alpha}$-EA	$PGF_{2\alpha}$-EA-d4
Stearoyl-EA	Stearoyl-EA-d3